JOURNAL OF THE AMERICAN WATER RESOURCES ASSOCIATION

Vol. 48, No. 6 AMERICAN WATER RESOURCES ASSOCIATION December 2012

PROJECTIONS OF 21ST CENTURY SIERRA NEVADA LOCAL HYDROLOGIC FLOW COMPONENTS USING AN ENSEMBLE OF GENERAL CIRCULATION MODELS[1]

Darren L. Ficklin, Iris T. Stewart, and Edwin P. Maurer[2]

ABSTRACT: Sierra Nevada snowmelt and runoff is a key source of water for many of California's 38 million residents and nearly the entire population of western Nevada. The purpose of this study was to assess the impacts of expected 21st Century climatic changes in the Sierra Nevada at the subwatershed scale, for all hydrologic flow components, and for a suite of 16 General Circulation Models (GCMs) with two emission scenarios. The Soil and Water Assessment Tool (SWAT) was calibrated and validated at 35 unimpaired streamflow sites. Results show that temperatures are projected to increase throughout the Sierra Nevada, whereas precipitation projections vary between GCMs. These climatic changes drive a decrease in average annual streamflow and an advance of snowmelt and runoff by several weeks. The largest streamflow reductions were found in the mid-range elevations due to less snow accumulation, whereas the higher elevation watersheds were more resilient due to colder temperatures. Simulation results showed that decreases in snowmelt affects not only streamflow, but evapotranspiration, surface, and subsurface flows, such that less water is available in spring and summer, thus potentially affecting aquatic and terrestrial ecosystems. Declining spring and summer flows did not equally affect all subwatersheds in the region, and the subwatershed perspective allowed for identification for the most sensitive basins throughout the Sierra Nevada.

(KEY TERMS: hydrologic cycle; climate variability/change; surface water hydrology; snow hydrology; precipitation; infiltration; evapotranspiration.)

Ficklin, Darren L., Iris T. Stewart, and Edwin P. Maurer, 2012. Projections of 21st Century Sierra Nevada Local Hydrologic Flow Components Using an Ensemble of General Circulation Models. *Journal of the American Water Resources Association* (JAWRA) 48(6): 1104-1125. DOI: 10.1111/j.1752-1688.2012.00675.x

INTRODUCTION

Changes to the quantity and timing of snowmelt-derived mountain runoff, which on a global scale provides water for one-sixth of the world's population, are thought to be among the most critical impacts expected from human-induced climate change for the 21st Century (e.g., Barnett *et al.*, 2005). The Sierra Nevada in California is an example of a snowmelt-driven hydrologic system that represents a key source of water and energy for many of California's 38 million residents and nearly the entire population of western Nevada. A large volume of this water comes from snowmelt originating at high elevations (Maurer, 2007), whereas the lowlands, and especially the

[1]Paper No. JAWRA-11-0117-P of the *Journal of the American Water Resources Association* (JAWRA). Received September 26, 2011; accepted April 23, 2012. **Discussions are open until six months from print publication**.

[2]Respectively, Postdoctoral Researcher (Ficklin) and Assistant Professor (Stewart), Department of Environmental Studies and Sciences, Santa Clara University, Santa Clara, California 95053; and Associate Professor (Maurer), Civil Engineering Department, Santa Clara University, Santa Clara, California 95053 (E-Mail/Ficklin: dficklin@scu.edu).

highly developed valley and coastal regions, are semi-arid or arid. Precipitation in this region is highly seasonal, with most precipitation coming during the winter season. Year-to-year variations in precipitation amounts vary greatly, with often just a few storms supplying the majority of water for a given water year (Ralph and Dettinger, 2011). Dry and drought years have also been a regular occurrence throughout the American West (Cook *et al.*, 2007). Therefore, rivers within the Sierra Nevada have been extensively developed for water resources through a statewide system of reservoirs, canals, and aqueducts. In fact, the Cosumnes River, located in the central Sierra Nevada, is the last larger free-flowing river in the western Sierra Nevada.

In spite of the extensive development, water resources remain scarce and management for human, agricultural, hydroelectric, and ecosystem needs is highly contested in the region (Gleick, 1993; Blumm and Schwartz, 2003). Water resources in California are highly dependent on the amount of snowpack within the Sierra Nevada, and therefore year-to-year as well as long-term changes in temperature and precipitation. Warmer winter and spring temperatures decrease the amount of precipitation coming as snow and result in a decreased snowpack that is melting earlier, resulting in a longer summer season with low flows (Knowles and Cayan, 2002; Stewart *et al.*, 2005; Coats, 2010). Precipitation decreases in winter and early spring are likely to exacerbate this effect, whereas precipitation increases during winter can mitigate the effects of warming by producing a larger snowpack that melts later in the year. Thus, changes such as those expected from climate change could potentially have a large effect on the amount of water available for public consumption, the agricultural and industrial sectors, energy production, and aquatic ecosystems. As a result, an understanding of the connection between climatic variations and climate change and the Sierra Nevada hydrology is of great interest.

Not surprisingly, then, the history and future of the Sierra Nevada hydrology have been studied extensively (e.g., Lettenmaier and Gan, 1990; Gleick and Chalecki, 1999; Miller *et al.*, 2003; Dettinger *et al.*, 2004; Hayhoe *et al.*, 2004; Van Rheenen *et al.*, 2004; Stewart *et al.*, 2005; Zhu *et al.*, 2005; Maurer, 2007; Young *et al.*, 2009; Null *et al.*, 2010; Coats *et al.*, 2012. Several of these studies (Dettinger *et al.*, 2004; Stewart *et al.*, 2005) found that warming over the past several decades has shifted snowmelt runoff timing to earlier in the year and contributed to less runoff during the summer season with the greatest water demands. These observed changes are likely to intensify with global changes (Stewart *et al.*, 2004; Christensen *et al.*, 2007).

Projections derived from General Circulation Models (GCMs) through the end of the century all show an increase in air temperature throughout the Sierra Nevada (e.g., Maurer, 2007; Cayan *et al.*, 2008; Ficklin *et al.*, 2012) by 1 to 4.5°C. Precipitation projections for the region, however, vary between GCMs, with some projecting increases and others projecting decreases. Assessments for the 21st Century have been produced for both the managed (e.g., Brekke *et al.*, 2004; Tanaka *et al.*, 2006; Vicuna *et al.*, 2007) and the unaltered (e.g., Maurer and Duffy, 2005; Maurer, 2007; Young *et al.*, 2009; Null *et al.*, 2010) Sierra Nevada hydrologic system. Simple temperature forcings with fixed increments of 2, 4, and 6°C while keeping precipitation constant were used in some studies (Miller *et al.*, 2003; Young *et al.*, 2009; Mehta *et al.*, 2011). The rationale for these is that mean values of projected precipitation changes are unknown or close to historical precipitation values (Dettinger, 2005; Maurer, 2007; Mehta *et al.*, 2011). However, simple temperature forcings do not necessarily capture the effects of combined temperature and precipitation changes, including changes in seasonality, asymmetric seasonal differences, and differential warming by region and/or elevation and extremes, which could be substantially different from simple temperature increases. This provided a motivation for using a suite of downscaled GCM projections as input to Sierra Nevada hydroclimate simulations. Furthermore, examining an ensemble of GCM projections allows some characterization of the uncertainty in the climate response to changing atmospheric concentrations of greenhouse gases. This uncertainty, with the uncertainty in the greenhouse gas levels themselves, are arguably the most important uncertainties in climate projections, especially at longer time scales out to year 2100 (e.g., Hawkins and Sutton, 2009, 2011).

Many of the Sierra Nevada climate change studies agree that an increase in temperature will lead to a shift in peak streamflow timing, decrease in mean annual flow, reduced snowpack, and an increase in snowmelt runoff. Using uniform temperature increases of 2, 4, and 6°C, Null *et al.* (2010) found that watersheds in the northern Sierra Nevada are most vulnerable to decreased annual streamflow, southern-central watersheds are more susceptible to changes in streamflow timing, and the central watersheds are more likely to have long periods of low flow. Miller *et al.* (2003) used six California watersheds to determine a range of hydrologic effects and found shifts of one to two months in mean monthly peak flow timing for temperature increases of 5°C. Using 11 GCMs with two emission scenarios, Maurer (2007) found that changes in the runoff center of mass are expected to shift from one to seven weeks by the end of the century. Most of these studies also agree that the largest changes in snowmelt due to climate change will be at the mid-range elevations of 1,500 to 3,000 m. For total percent change in snowmelt, the largest changes occur at the lower elevations of 0 to 1,500 m (e.g., Maurer, 2007; Young *et al.*, 2009). None of these previous studies, except for Young *et al.* (2009), have assessed the impact of climate change on hydrology within the often ecologically important, smaller subwatersheds of the Sierra Nevada. Although Young *et al.* (2009) evaluated future changes in snowmelt and streamflow timing at the subwatershed scale, they used fixed temperature increases, focused on the western Sierra Nevada, and did not include individual hydrologic components (groundwater, soil water flow, surface runoff, evapotranspiration) change with climatic change in their study. As eastern Sierra Nevada watersheds are at higher elevation and have a different geologic makeup than western Sierra Nevada watersheds, the future hydrologic response in those regions could substantially differ. The effects of climate change on individual hydrologic components in the Sierra Nevada have yet to be analyzed.

Large-scale hydrologic modeling is well suited for studies concerned with inflows to water supply reservoirs. Assessing changes in local flow regimes for aquatic habitats, however, requires simulations and analysis on the subwatershed or reach scale, as many aquatic species in the Sierra Nevada are isolated at all elevations in first- and second-order streams, and may even be limited in distribution to small headwater streams (e.g., Wiggins, 1990; Erman and Nagano, 1992; Hershler, 1994). The goal of this study then is to assess the effects of expected climatic changes in the eastern and western Sierra Nevada for all hydrologic flow components and the subwatershed scale, for a suite of 16 GCMs and two different emission scenarios. Our approach is new in that we seek to understand how earlier snowmelt runoff impacts all hydrologic components of river flow, including precipitation, river discharge, and the hydrologic components of discharge resulting from snowmelt, surface runoff, subsurface runoff, groundwater flow, and evapotranspiration. We also apply the Soil and Water Assessment Tool (SWAT) (Arnold *et al.*, 1998), which has been successfully applied throughout the world (Gassman *et al.*, 2007) but has yet to be applied in the Sierra Nevada, to simulate changes in Sierra Nevada hydrology from climate change forcings. For all Sierra Nevada subwatersheds (a total of 498), we explore the spatially varying changes in streamflow and snowmelt in the spring and summer seasons under climate change. Through this approach, we identify drainage watersheds or regions that are most vulnerable to future changes in climate.

MATERIALS AND METHODS

Study Area

The area of focus in this study is the Sierra Nevada in California (Figure 1). The Sierra Nevada has a general north to south orientation, where the western Sierra Nevada rivers generally flow westward into the Sacramento and San Joaquin Rivers, which then flow into the Sacramento-San Joaquin River Delta, and the eastern Sierra Nevada rivers generally flow eastward into terminal lakes within the Great Basin of Nevada. The southern portion of the Sierra Nevada has a higher elevation of approximately 4,400 m at the peak, whereas the northern Sierra Nevada peaks are generally below 3,000 m (Figure 1).

In this study, the modeled outlets for the eastern Sierra Nevada rivers are located within California, where a large portion of their source water from snowmelt is located. The western watersheds modeled for this study span the Sacramento River to the north and the Kern River to the south (Figure 1). The eastern watersheds span from the Truckee River to the north and Rush Creek to the south (Figure 1). Four major watersheds are assessed for the Westside Sierra Nevada (Sacramento River, American River, San Joaquin River, and Kern River) and the Eastside Sierra

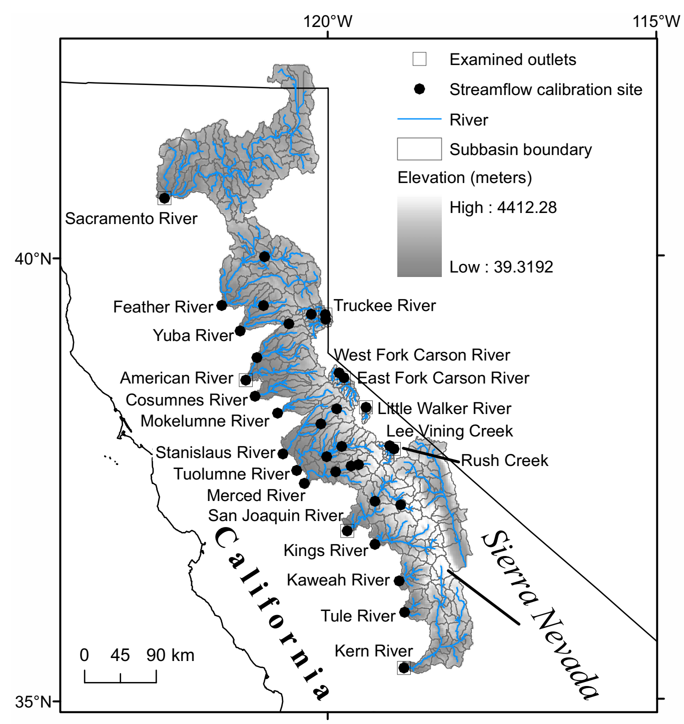

FIGURE 1. Sierra Nevada Study Area Showing Streamflow Calibration Sites and Examined Outlets.

Nevada (Truckee River, East Fork Carson River, Little Walker River, and Rush Creek). For the Westside Sierra Nevada mountain range, the top five land covers in terms of area are evergreen forest (51% of the total Westside area), brush rangeland (29.4%), grass rangeland (8.2%), Southwestern United States (U.S.) range (4.6%), and open water (1.9%) (USGS, 2007). For the Eastside Sierra Nevada, the top five land covers are brush rangeland (44.6%), evergreen forest (43.3%), Southwestern U.S. range (5.0%), grass rangeland (2.9%), and open water (1.5%) (USGS, 2007). Soil types vary throughout the Sierra Nevada, with a total of 110 soil types within the study area. Generally, soils found within the Sierra Nevada are thin and rocky and largely underlain by granite. In general, watersheds within the Sierra Nevada are expansively developed for water resources. Physical characteristics of the eight major watersheds assessed in this study can be found in Table 1.

The Sierra Nevada exhibits a typical Mediterranean climate below approximately 2,000 m and a boreal climate at the high elevations. Precipitation during the wet season falls as rain in the lower elevations and snow in the higher elevations with a snowline of approximately 1,000 m above sea level. Precipitation throughout the Sierra Nevada is highly variable with an annual average of 100 cm/yr from 1950 to 2005. The highest average annual precipitation in the Sierra Nevada from 1950 to 2005 is 180 cm/yr and is found in the high elevations of the Yuba River watershed. The lowest average annual precipitation in the Sierra Nevada is 30 cm/yr and occurs in the low elevations of the Kern River watershed. The snowpack of the Sierra Nevada stores a large volume of water throughout the winter and spring and is released as snowmelt during the spring and summer. Increasing temperatures decrease the fraction of precipitation that comes as snow, resulting in a smaller snowpack. Warmer spring temperatures and a smaller snowpack both contribute to earlier snowmelt runoff.

SWAT Hydrologic Model

SWAT is a river basin-scale model designed to simulate watershed and water-quality processes. SWAT simulates the entire hydrologic cycle, including surface runoff, lateral soil flow, evapotranspiration, infiltration, deep percolation, and groundwater return flows. For this study, surface runoff was estimated using the Soil Conservation Service Curve Number (SCS, 1984) and evapotranspiration was estimated using the Penman-Monteith method (Penman, 1956; Monteith, 1965). Relative humidity and solar radiation are generated using the SWAT weather generator. Soil water can be removed by evapotranspiration, deep percolation for aquifer recharge, or move laterally in the soil column for streamflow contribution. Groundwater return flow was estimated based on the groundwater balance, where shallow and deep aquifers can contribute to streamflow. For this study, we combine the soil water contribution and the groundwater return flows into a single volume termed "subsurface flow." The model was run at a monthly time step for historic (1950-2005) and future climate scenarios. A full description of SWAT can be found in Neitsch *et al.* (2005).

SWAT uses a temperature index-based approach to estimate snow accumulation and snowmelt processes (Neitsch *et al.*, 2005). Precipitation is assumed to fall as snow if the temperature is below a user-defined temperature threshold. Snowpack temperature is based on the average daily temperature and the previous day's snowpack temperature and is defined by a snowpack temperature lag factor. Snowmelt is estimated as a linear function of the differences between the average of the daily maximum air and snowpack temperatures and the user-defined snowmelt temperature threshold. The melt factor is estimated based on the maximum and minimum snowmelt rates for the summer and winter solstices, respectively. SWAT uses an aerial snow coverage distribution curve to estimate the total melt water produced based on the

TABLE 1. Physical Characteristics of the Selected Eastern and Western Sierra Nevada Watersheds.

Watershed	Area (km^2)	Elevation Range (m)	Median Elevation (m)	Watershed Centroid (°)	Slope (%)	Runoff Coefficient (R/P)
Sacramento River	18,835.7	191-4,298	1,334	41.20, −121.24	13.0	0.18
American River	4,815.5	39-3,155	1,068	38.94, −120.66	29.3	0.07
San Joaquin River	4,333.6	91-4,226	2,265	37.34, −119.19	31.2	0.08
Kern River	6,091.9	134-4,409	1,651	35.91, −118.38	32.2	0.07
Truckee River	1,098.3	1,569-3,231	1,856	39.39, −120.15	21.3	0.09
East Fork Carson River	716.1	1,645-3,478	2,243	38.61, −119.72	31.8	0.05
Little Walker River	164.9	2,018-3,522	2,367	38.31, −119.45	24.9	0.04
Rush Creek	284.3	2,032-3,947	2,357	37.83, −119.13	29.6	0.06

Notes: R, runoff volume; P, precipitation volume.

total areal snow cover of the watershed. The curve is defined by the maximum snow cover at 95% snow cover and at 50% areal snow cover content (Neitsch *et al.*, 2005). Snowmelt is treated the same as rainfall for estimating surface runoff and infiltration.

The SWAT snow routine also includes elevation bands with each subwatershed, as modified by Fontaine *et al.* (2002). The addition of elevation bands allows SWAT to better represent the distribution of precipitation and temperature over areas that contain large elevation changes. Further, the addition of elevation bands allow for better representation of precipitation and temperature lapse rates. Hanson *et al.* (2004) reported that the difference of temperature between low and high elevation sites vary between 4°C/km in the winter and 7°C/km in the summer. The precipitation lapse rate will vary from region to region (Fontaine *et al.*, 2002) and, for this study, the lapse rate values varied for each subwatershed from −10 to −1°C/km for temperature and 100 to 1,000 mm/km depending on calibration. This study used four elevation bands within each subwatershed.

Some simplifying assumptions employed in this study should be recognized. Alteration of land use such as urbanization, deforestation/forestation, irrigation of desert lands for crops, and the removal of wetlands can have significant implications for the hydrologic cycle. However, this study assumes that land use will stay constant throughout the 21st Century as plausible land-use change scenarios for these mountain basins were not available. Further, SWAT has a simplified groundwater routine where groundwater contributes to streamflow only if the water stored in the shallow aquifer exceeds a user-defined water table height (Neitsch *et al.*, 2005). Lastly, we assume a constant atmospheric CO_2 concentration within SWAT throughout all model simulations. The effect of CO_2 on plant growth and transpiration, and thus evapotranspiration, is significant within highly vegetated watersheds (e.g., Morison and Gifford, 1983; Medlyn *et al.*, 2001; Gedney *et al.*, 2006; Ficklin *et al.*, 2009).

Input Data

Human-induced climatic projections from the 16 GCMs given in Table 2 and two Intergovernmental Panel on Climate Change (IPCC) emission scenarios (A2 and B1) were used to drive SWAT. These emission scenarios were selected to represent a more pessimistic case (higher greenhouse gas emissions) and an optimistic case (lower emissions) scenarios, respectively. However, Raupach *et al.* (2007) indicate that current CO_2 emissions are greater than the projected IPCC A2 emission scenario pathway, highlighting that the A2 emission scenario cannot be considered as a worst-case scenario. Data include daily precipitation, maximum and minimum temperature, and wind speed from 1950 to 2099. It is recognized that, in preparation for the planned 2012 Fifth Assessment of the IPCC, there are new emissions scenarios (termed representative concentration pathways) that have

TABLE 2. Climate Models Used in the Study.

Model No.	IPCC Model ID	Modeling Group and Country	Reference
1	BCCR-BCM 0.1	Bjerknes Centre for Climate Research	Furevik *et al.*, 2003
2	CGCM3.1 (T47)	Canadian Centre for Climate Modeling & Analysis	Flato and Boer, 2001
3	CNRM-CM3	Météo-France/Centre National de Recherches Météorologiques, France	Salas-Mélia *et al.*, 2005
4	CSIRO-Mk3.0	CSIRO Atmospheric Research, Australia	Gordon *et al.*, 2002
5, 6	GFDL-CM2: 0.1, 1.1	U.S. Department of Commerce/NOAA/Geophysical Fluid Dynamics Laboratory, U.S.	Delworth *et al.*, 2005
7	GISS-ER	NASA/Goddard Institute for Space Studies, U.S.	Russell *et al.*, 1999, 2000
8	INM-CM3.0	Institute for Numerical Mathematics, Russia	Diansky and Volodin, 2002
9	IPSL-CM4	Institut Pierre Simon Laplace, France	IPSL, 2005
10	MIROC3.2	Center for Climate System Research (The University of Tokyo), National Institute for Environmental Studies, and Frontier Research Center for Global Change (JAMSTEC), Japan	K-1 Model Developers, 2004
11	ECHO-G	Meteorological Institute of the University of Bonn, Meteorological Research Institute of KMA	Legutke and Voss, 1999
12	ECHAM5/MPI-OM	Max Planck Institute for Meteorology, Germany	Jungclaus *et al.*, 2006
13	MRI-CGCM2.3.2	Meteorological Research Institute, Japan	Yukimoto *et al.*, 2001
14	CCSM	National Center for Atmospheric Research, U.S.	Kiehl *et al.*, 1998
15	PCM	National Center for Atmospheric Research, U.S.	Washington *et al.*, 2000
16	UKMO-HadCM3	Hadley Centre for Climate Prediction and Research/Met Office, UK	Gordon *et al.*, 2000

been developed (Moss *et al.*, 2010); however, as of this writing comprehensive GCM output is not available for these new scenarios. The GCM data were obtained from World Climate Research Programme's (WCRP's) Coupled Model Intercomparison Project phase 3 (CMIP3) (Meehl *et al.*, 2007a). All GCM output was interpolated onto a common 2° grid, and statistically downscaled using the well-established bias-correction and spatial disaggregation (BCSD) method of Wood *et al.* (2002, 2004). Data downscaled using the BCSD method have been widely used for studies in California and the western U.S. (e.g., Hayhoe *et al.*, 2004; Van Rheenen *et al.*, 2004; Maurer, 2007; Barnett *et al.*, 2008; Cayan *et al.*, 2008; Maurer *et al.*, 2010a). Although the uncertainties associated with the response of the climate to changes in atmospheric composition may be much larger than that represented by the ensemble of GCMs (Roe and Baker, 2007; Sanderson *et al.*, 2007), the use of ensembles allows the assessment of some of this uncertainty around the central tendency, and provides more quantitative climate change information for impact studies (Meehl *et al.*, 2007b).

SWAT input parameter values from topography, land cover, and soils data were compiled using databases from governmental agencies. A 30-m digital elevation model was obtained from the U.S. Geological Survey (USGS) for watershed and stream delineation and estimation of stream slopes. The 2001 National Land Cover database was used to define land cover. We assume that land use remains constant for all simulations. Soil properties were established from the State Soil Geographic database (STATSGO) (USDA-SCS, 1993). Natural flow data for streamflow calibration were gathered from the California Data Exchange Center (CDEC) and USGS. The CDEC natural flow data are derived from climate/runoff relationships and is the streamflow that would occur if no reservoirs were present and no streamflow diversions were occurring. The USGS streamflow data were selected for those at sites that are unimpaired. About 1/8° (~12 km) spatial resolution daily climate data from 1949 to 2005, including precipitation, maximum and minimum temperature, and wind speed, were obtained from gridded observed meteorological data (Maurer *et al.*, 2002).

SWAT Model Calibration and Validation Procedure

An automated calibration technique using the program Sequential Uncertainty Fitting Version 2 (SUFI-2) (Abbaspour *et al.*, 2007) was used to calibrate the SWAT model at 35 streamflow outlets within the Sierra Nevada (Figure 1). These outlets include gauges at the reservoir inlets at the base of the Sierra Nevada and also within the central and higher elevations. Sensitive initial and default parameters relating to hydrology were varied simultaneously until an optimal solution was met. It should be noted that due to the automatic calibration process, where each streamflow gauge is weighted equally toward the final Nash-Sutcliffe objective function, and the use of global parameters in SWAT, calibration results for individual gauges may be less optimal when compared with calibrations for individual watersheds. The most sensitive calibration parameters were mostly related to snowfall/snowmelt generation (snowfall temperature [SFTMP.bsn in SWAT], snowmelt base temperature [SMTMP.bsn], snowmelt temperature lag factor [TIMP.bsn], melt factor for snow on December 21 [SMFMN.bsn], and melt factor for snow on June 21 [SMFMX.bsn]) and surface runoff/infiltration/groundwater flow generation (Curve Number [CN2.mgt], alpha base-flow factor [ALPHA_BF.gw], groundwater delay [GW_DELAY.gw], and soil hydraulic conductivity [Sol_K.sol]). Three optimization criteria were used to assess model performance: (1) the coefficient of determination (R^2), (2) a modified efficiency criterion (ϕ), and (3) the Nash-Sutcliffe coefficient (NS) (Nash and Sutcliffe, 1970). ϕ is a slightly modified version of the efficiency criterion defined by Krause *et al.* (2005) where the coefficient of determination, R^2, is multiplied by the slope of the regression line, b. This function allows accounting for the discrepancy in the magnitude of two signals (captured by b) as well as their dynamics (captured by R^2). For ϕ, a perfect simulation is represented by a value of 1. A split-sample approach was used for calibration and validation. The calibration and validation years differed at each outlet depending on streamflow data availability (Tables 3 and 4). A model warm-up time period of one year was used from 1949 to 1950.

Statistical Analyses

The impact of potential climate change on streamflow was evaluated by comparing simulations using the GCMs in Table 2 under the B1 and A2 emission scenarios for two future time periods: 2050s (2040-2069) and 2080s (2070-2099) to those of the historical time period (1960-2005). For the monthly streamflow time series, t-tests for dependent samples were used to compare climate change and present-day scenarios with a target level of significance of $\alpha = 0.05$. Spring and summer seasons for the spatial analysis are defined as April, May, June and July, August, September, respectively.

To assess differences in watershed climate-change vulnerability, a factor termed the "r-factor" was used

TABLE 3. Eastern Sierra Nevada Monthly Streamflow Calibration and Validation Statistics.

			Calibration				Validation			
Site	Latitude	Longitude	Years	R^2	NS	ϕ	Years	R^2	NS	ϕ
Sagehen Creek	39.43	−120.24	1970-1974; 2002	0.73	0.66	0.68	2003-2005	0.64	0.54	0.53
Truckee River	39.43	−120.03	1950-1979	0.81	0.79	0.71	1980-2005	0.73	0.71	0.56
Gray Creek	39.37	−120.03	2001-2003	0.90	0.79	0.76	2004-2005	0.95	0.88	0.88
West Fork Carson River	38.77	−119.83	1950-1979	0.79	0.65	0.72	1980-2005	0.70	0.68	0.57
East Fork Carson River	38.71	−119.77	1960-1985	0.90	0.84	0.83	1986-2005	0.82	0.76	0.82
Little Walker River	38.38	−119.45	1950-1974	0.68	0.61	0.58	1975-1997	0.65	0.52	0.58
Lee Vining Creek	37.98	−119.14	1950-1974	0.86	0.85	0.78	1975-1992	0.91	0.81	0.79
Rush Creek	37.91	−119.05	1950-1974	0.81	0.81	0.69	1975-1993	0.88	0.80	0.81

Notes: R^2, coefficient of determination; NS, Nash-Sutcliffe coefficient; ϕ, modified efficiency criterion.

TABLE 4. Western Sierra Nevada Monthly Streamflow Calibration and Validation Statistics.

			Calibration				Validation			
Site	Latitude	Longitude	Years	R^2	NS	ϕ	Years	R^2	NS	ϕ
Sacramento River	40.72	−122.42	1950-1979	0.81	0.80	0.74	1980-2005	0.80	0.76	0.75
Indian Creek	39.52	−121.55	1950-1974	0.75	0.72	0.45	1975-1993	0.80	0.77	0.59
Feather River	39.53	−120.94	1950-1979	0.88	0.87	0.70	1980-2005	0.93	0.89	0.81
North Yuba River	39.24	−121.27	1950-1974	0.81	0.78	0.62	1975-1995	0.85	0.74	0.76
South Yuba River	38.94	−121.02	1950-1974	0.82	0.78	0.75	1975-1994	0.86	0.83	0.60
Yuba River	38.68	−121.18	1950-1979	0.85	0.84	0.66	1980-2005	0.91	0.89	0.74
North Fork American River	38.50	−121.04	1950-1974	0.84	0.77	0.75	1975-1995	0.82	0.80	0.63
American River	38.31	−120.72	1950-1979	0.85	0.85	0.68	1980-2005	0.89	0.88	0.71
Consumnes River	38.19	−120.10	1950-1979	0.87	0.78	0.80	1980-2005	0.87	0.83	0.83
Middle Fork Stanislaus River	37.85	−120.64	1950-1975	0.87	0.84	0.61	1975-1994	0.82	0.78	0.53
Mokelumne River	37.94	−119.80	1950-1979	0.60	0.59	0.39	1980-2005	0.73	0.72	0.58
Middle Fork Stanislaus River	37.67	−120.44	1950-1974	0.78	0.76	0.52	1975-1995	0.68	0.66	0.52
Tuolumne River	37.72	−119.67	1950-1974	0.75	0.74	0.62	1975-1992	0.83	0.76	0.80
Stanislaus River	37.52	−120.33	1950-1979	0.82	0.77	0.51	1980-2005	0.89	0.85	0.65
South Fork Tuolumne River	37.32	−119.33	1950-1979	0.67	0.65	0.51	1980-2001	0.65	0.61	0.52
Merced River	37.27	−118.97	1950-1979	0.74	0.74	0.50	1980-2005	0.83	0.81	0.58
Merced River	36.98	−119.72	1950-1974	0.77	0.76	0.62	1975-1995	0.79	0.78	0.57
Tuolumne River	36.83	−119.34	1950-1979	0.85	0.84	0.65	1980-2005	0.88	0.85	0.75
South Fork Merced River	36.41	−119.00	1951-1965	0.72	0.65	0.52	1966-1975	0.77	0.72	0.56
Merced River	36.06	−118.92	1950-1979	0.76	0.47	0.72	1980-2005	0.81	0.66	0.70
San Joaquin River	35.43	−118.95	1950-1966	0.85	0.78	0.79	1967-1980	0.87	0.84	0.66
South Fork San Joaquin River	37.82	−120.01	1950-1966	0.74	0.68	0.69	1967-1980	0.69	0.68	0.49
San Joaquin River	40.08	−120.93	1950-1979	0.87	0.85	0.65	1980-2005	0.88	0.83	0.68
Kings River	39.32	−120.56	1950-1979	0.92	0.90	0.81	1980-2005	0.90	0.86	0.71
Kaweah River	38.36	−119.87	1950-1979	0.87	0.85	0.77	1980-2005	0.91	0.87	0.79
Tule River	37.65	−119.89	1950-1979	0.79	0.65	0.73	1980-2005	0.78	0.63	0.39
Kern River	37.73	−119.56	1950-1979	0.75	0.64	0.67	1980-2005	0.82	0.80	0.61

Notes: R^2, coefficient of determination; NS, Nash-Sutcliffe coefficient; ϕ, modified efficiency criterion.

to assess the difference in sensitivities between watersheds (Abbaspour *et al.*, 2007). For this study, we define "watershed sensitivity" as the potential for the watershed to be affected by climate change, even though the median streamflow value indicated moderate change. The *r*-factor is calculated by taking the average streamflow interquartile range (IQR) (third quartile minus the first quartile) of all months and then dividing this value by the standard deviation of the IQR values. For example, the 2080s time period will have 360 IQR values (30 years with 12 months/yr). The *r*-factor is the average value of the 360 IQRs divided by the standard deviation of the 360 IQRs. The width between the streamflow quartiles measures the range of streamflow predictions with changes in climate, while dividing by the standard deviation normalizes the *r*-factor so that it is comparable between watersheds.

RESULTS AND DISCUSSION

SWAT Model Calibration and Validation

Streamflow outlets throughout the Sierra Nevada were calibrated with monthly unimpaired streamflow estimates. Full calibration and validation statistics are shown in Tables 3 and 4. Overall, the calibrated SWAT model generally performed well, with an average NS coefficient of 0.75 for the calibration period and 0.77 for the validation period. The NS standard deviation for the calibration and validation periods was 0.1. R^2 statistics also indicate a good relationship between observed and simulated streamflow values, with an average R^2 of 0.80 and 0.82 for the calibration and validation periods, respectively, and a standard deviation of 0.1. Average ϕ for model calibration and validation was 0.66, suggesting an overall underprediction of streamflow. The model efficiency statistics are lower than those of Young *et al.* (2009), which is likely due to the use of global model parameters in SWAT, but well within the range-acceptable calibration metrics established by Moriasi *et al.* (2007). Some parameters in SWAT such as the rain to snow temperature threshold have a single value for an entire watershed. Although the use of a single value may be apt for smaller watersheds, global parameters may need to vary for different regions in larger watersheds. Additionally, our model efficiency statistics include both major outlet and headwater gauges, compared with only major outlet gauges in Young *et al.* (2009). Model statistic discrepancies between the calibration and validation time periods may be explained by the use of NLCD data produced in 2001 throughout the model simulation years of 1950-2005, as differences in land use between calibration and validation periods may have an effect on the streamflow results.

For further model validation, we compared the annual percentage of simulated hydrologic components with observed hydrologic component data from Conklin and Liu (2006) at two locations within the Merced River watershed. The locations are the Briceburg (USGS Gauge ID # 11268200) and Happy Isle (USGS Gauge ID # 11264500) USGS-gauging stations, both of which are located on the Merced River. Based on observational data at the Briceburg station, the average annual hydrologic component streamflow contribution was 30% surface runoff and 70% for subsurface flow (as defined within this study), compared with the SWAT-simulated values of 27% for surface flow and 73% for subsurface flow. For the Happy Isle station, observations show that surface runoff and subsurface flow were 50% of the average annual streamflow contribution, compared with SWAT-simulated values of 35 and 65% for surface runoff and subsurface flow, respectively. Thus, we suggest that the SWAT-simulated values are simulating reasonable hydrologic component estimates.

GCM Projections for the Sierra Nevada

Figures 2 and 3 present GCM-projected changes in annual temperature and precipitation, respectively, between the historic and 2080s for the 20, 50 (median), and 80% quantiles. Figure 4 presents the median GCM projections for the transects displayed in Figures 2 and 3. Average end-of-the-century annual temperature is expected to be slightly higher in the southern Sierra Nevada by approximately 0.3°C for the B1 scenario and 0.4°C for the A2 scenario (Figure 4). The quantiles also show a southerly trend increase in average end-of-the-century annual temperature change (not shown). Although the difference in temperature changes between the northern and southern Sierra Nevada appear slight, an average 0.3 or 0.4°C increase may be a product of warmer periods significant enough to push an aquatic ecosystem over its temperature threshold or shift precipitation from snow to rain. Projected end-of-the-century median precipitation is highly variable from north (N) to south (S) in the Sierra Nevada (Figure 4). There is, however, a clear decreasing trend for the median of both emission scenarios. For the B1 scenario, precipitation decreases by −3.1% from N to −9.1% S. For the A2 scenario, precipitation decreases by approximately −5.5% from N to −14.5% S, with a sharp increase at the very southern end of the Sierra Nevada (Figure 4). For precipitation, the quantile trends remain similar as projected temperature changes, with the most extreme changes projected for the southern Sierra Nevada (not shown).

Our analysis of the GCM-based climatic projections suggests that the 21st Century warming trend in annual average temperature increases from west to east (Figures 2 and 3). On average, temperature increases from approximately 2.2 to 2.4°C for the B1 scenario and 4.0 to 4.2°C for the A2. End-of-the-century precipitation projections are highly variable between the west-east transects. Overall, larger precipitation decreases are projected, based on the ensemble median, at lower elevations than further upslope, as the large-scale changes are proportionately applied to climatological precipitation patterns in the downscaling method. The largest ensemble median-projected precipitation decreases are found in the southern G-H transect with average decreases of approximately −13%. The northern C-D transect has high variability due to large orographic differences in the Upper Sacramento River watershed. It is important to note that the median GCM projection shows a decrease in precipitation throughout the Sierra Nevada.

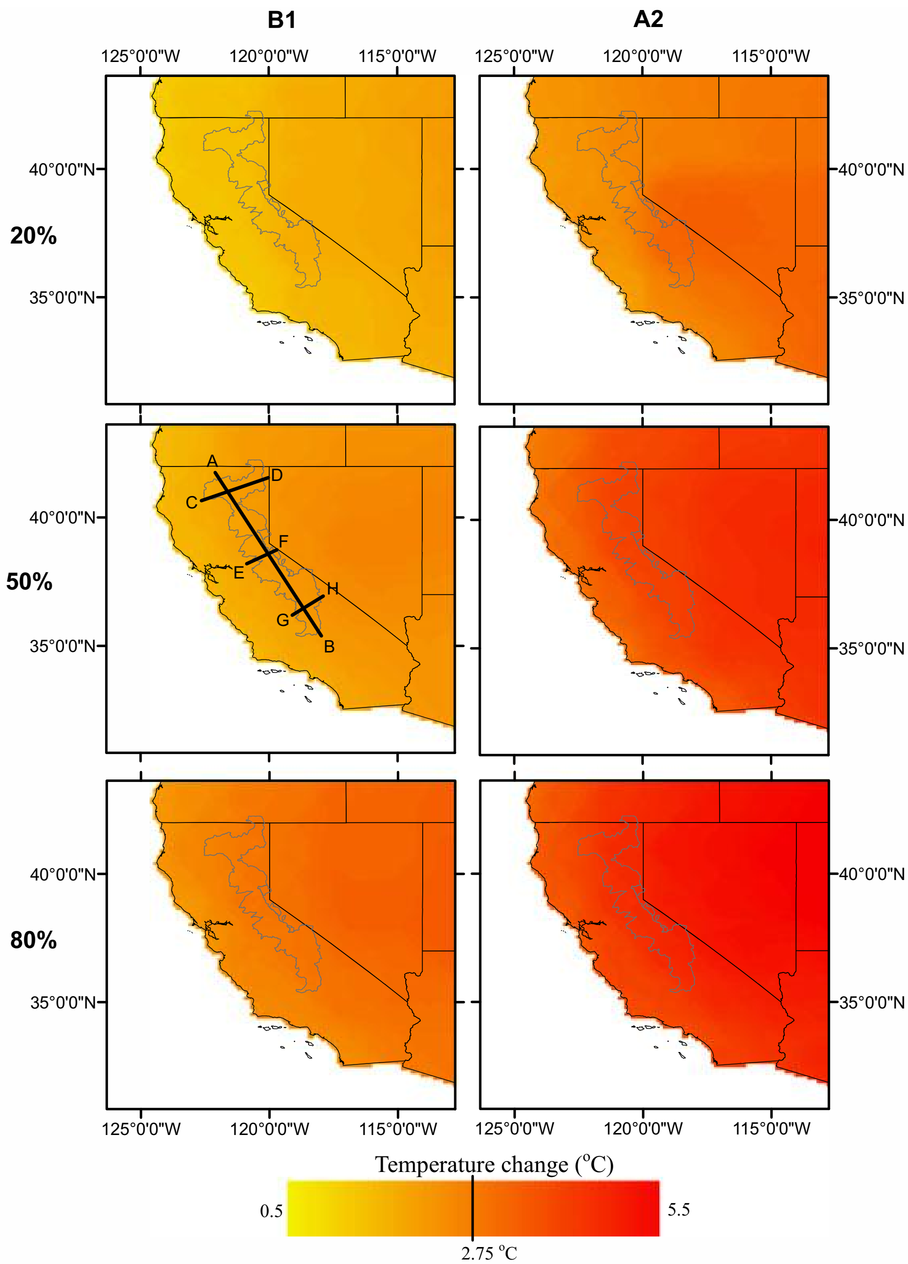

FIGURE 2. Quantiles of the Projected Annual Temperature Change of the California Region. The gray outline shows the location of the Sierra Nevada study site and the black lines show the location of the transects.

Future Hydrology in the Sierra Nevada

Future hydrology in the Sierra Nevada was assessed for eight major eastern and western Sierra Nevada watersheds and the subwatershed scale.

Major Eastern and Western Sierra Nevada Watersheds

The eight major Sierra Nevada watersheds analyzed for this study are the Sacramento River, American River, San Joaquin River, Kern River, Truckee River, East Fork Carson River, Little Walker River, and Rush Creek.

Average Median Monthly Streamflow

Compared with the historical period, the snowmelt runoff pulse for all the eight major outflows is projected to arrive increasingly earlier through the 21st Century, with a concurrent extension of the summer low-flow period for both the low and high emission

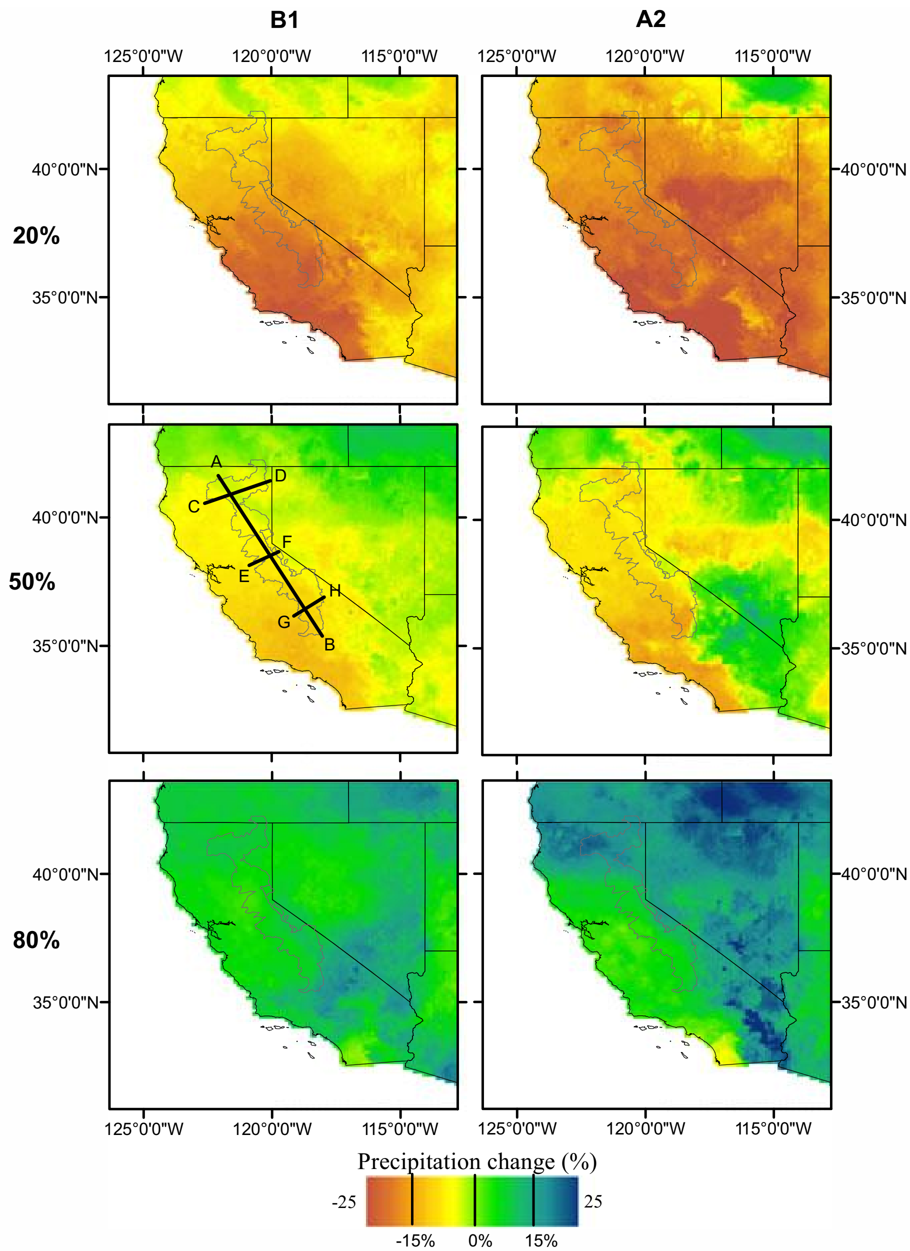

FIGURE 3. Quantiles of the Projected Annual Precipitation Change of the California Region. The gray outline shows the location of the Sierra Nevada study site and the black lines show the location of the transects.

scenarios. For comparison, average median monthly streamflow projections for eight major eastern and western Sierra Nevada watersheds are plotted in Figures 5 and 6. These results are in agreement with other studies (e.g., Miller *et al.*, 2003; Young *et al.*, 2009; Null *et al.*, 2010), where a shift of peak streamflow and annual hydrograph center of timing (Stewart *et al.*, 2004) from one to two months earlier is expected under future climate change scenarios. Of the eight major watersheds analyzed, only the East Fork Carson River and Little Walker River watersheds during the 2080s for the A2 scenario were found not to be statistically significantly different from the historical time period using a two-tailed t-test ($p > 0.05$) for the average median monthly streamflow projections (Table 5). The East Fork Carson and Little Walker River watersheds were not significantly different from the historical time period largely due to only slight changes in average annual precipitation, which decreased <6% compared with the historical time period. This slight decrease in precipitation did not change the streamflow distribution, but rather shifted the streamflow values forward in time.

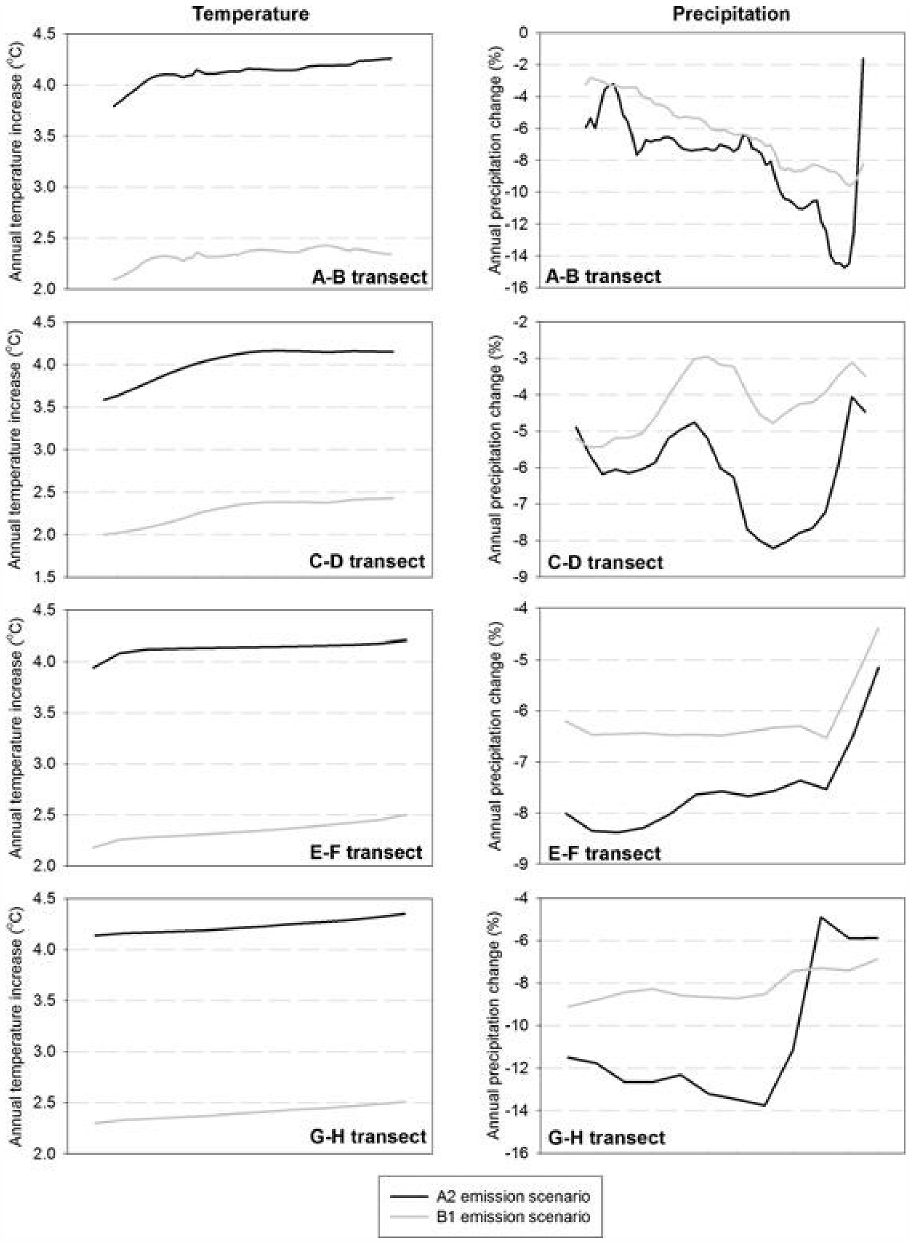

FIGURE 4. Annual Temperature and Precipitation Changes for the B1 and A2 Emission Scenario of the Transects Shown in Figure 3.

There was considerable variability in average median monthly streamflow changes between watersheds, largely due to differences in watershed area and elevation, as well as precipitation and temperature projections (Table 1 and Figures 2 and 3). Based on average median monthly flow change between the 2080s A2 scenario and the historical time period, the Kern River and San Joaquin watersheds are projected to have the largest decreases in average median monthly streamflow at −25.3 and −21.5%, respectively, relative to the historical time period (Table 5). This is due to the large decreases in projected annual precipitation and increases in average annual temperature (Figures 2 and 3), as well as their dependence on snowmelt for streamflow generation. The greatest snow accumulation occurs in the central and southern Sierra Nevada, whereas the greatest total liquid precipitation occurs in the northern Sierra Nevada based on climatological data. Further, the Kern and San Joaquin River watersheds contain some of the highest elevations in the Sierra Nevada where snow accumulation is prominent (Table 1).

On average, the western Sierra Nevada watersheds showed the largest average median monthly streamflow change with a −18% decrease compared

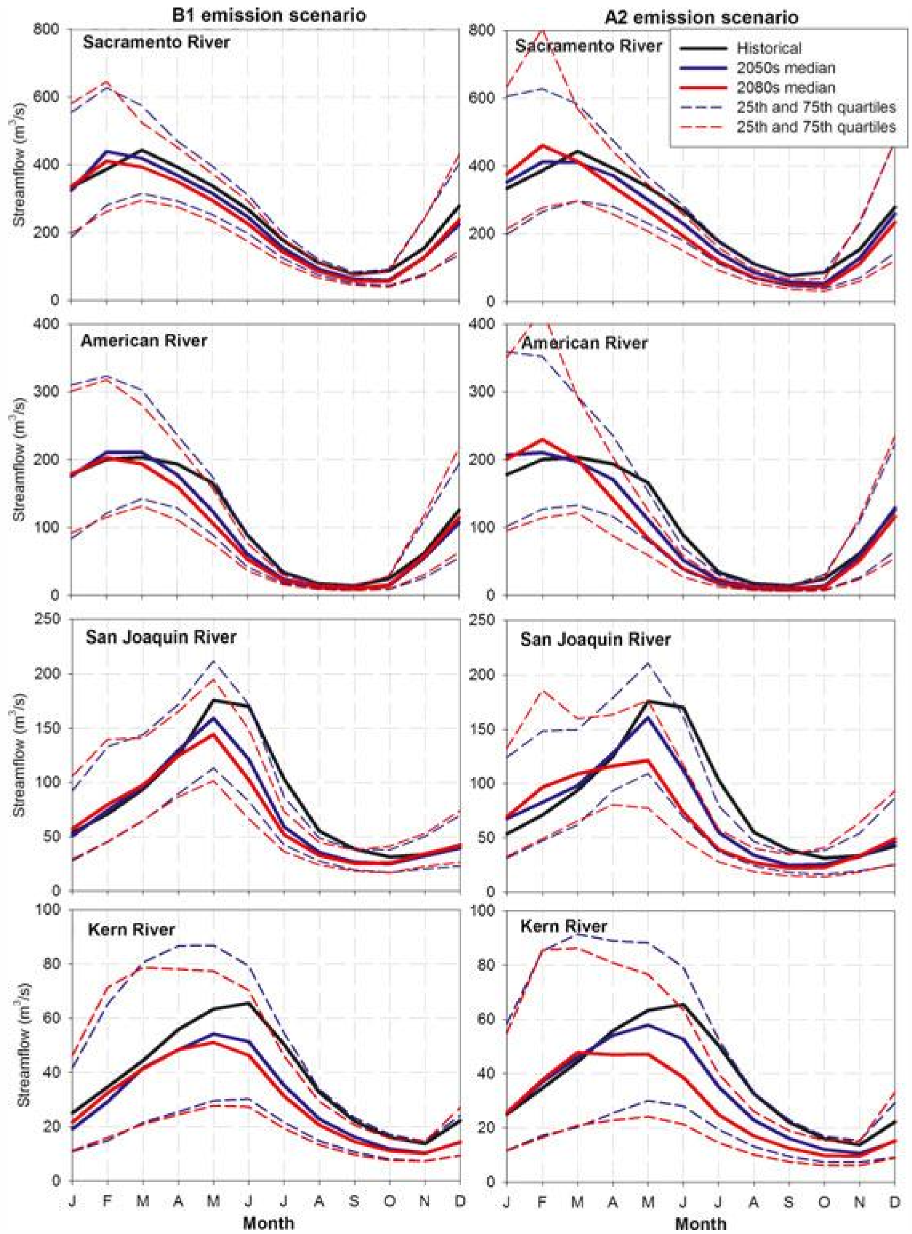

FIGURE 5. Average Median and Quartile Monthly Streamflow Projections for the 2050s and 2080s Under Each Emission Scenario for the Selected Western Sierra Nevada Watersheds.

with −13% decrease for the eastern watersheds, suggesting that from the median projections, the high elevation watersheds of the eastern Sierra Nevada are more resilient to climate changes. Eastern Sierra Nevada watersheds, however, exhibited greater variability, which is likely due to their lower runoff coefficient (runoff volume divided by precipitation volume; not shown). Wigley and Jones (1985) showed that percent changes in streamflow are amplified for watersheds with low runoff coefficients. Additionally, based on the average median monthly percent changes, the northern Sierra Nevada watersheds (Sacramento, American, Truckee, and East Fork Carson Rivers) were less affected by climate change than the southern Sierra Nevada watersheds (Table 5). These watersheds are less dependent on snowmelt for streamflow generation, and thus less affected by increases in temperature, and are therefore more resilient to changes in climate not driven by significant changes in precipitation amounts or timing.

Of the eight major watersheds, the East Fork Carson River watershed was found to be the most sensitive to climate change with an *r*-factor of 1.78, followed by San Joaquin River watershed (1.74), Little Walker River watershed (1.67), Kern River

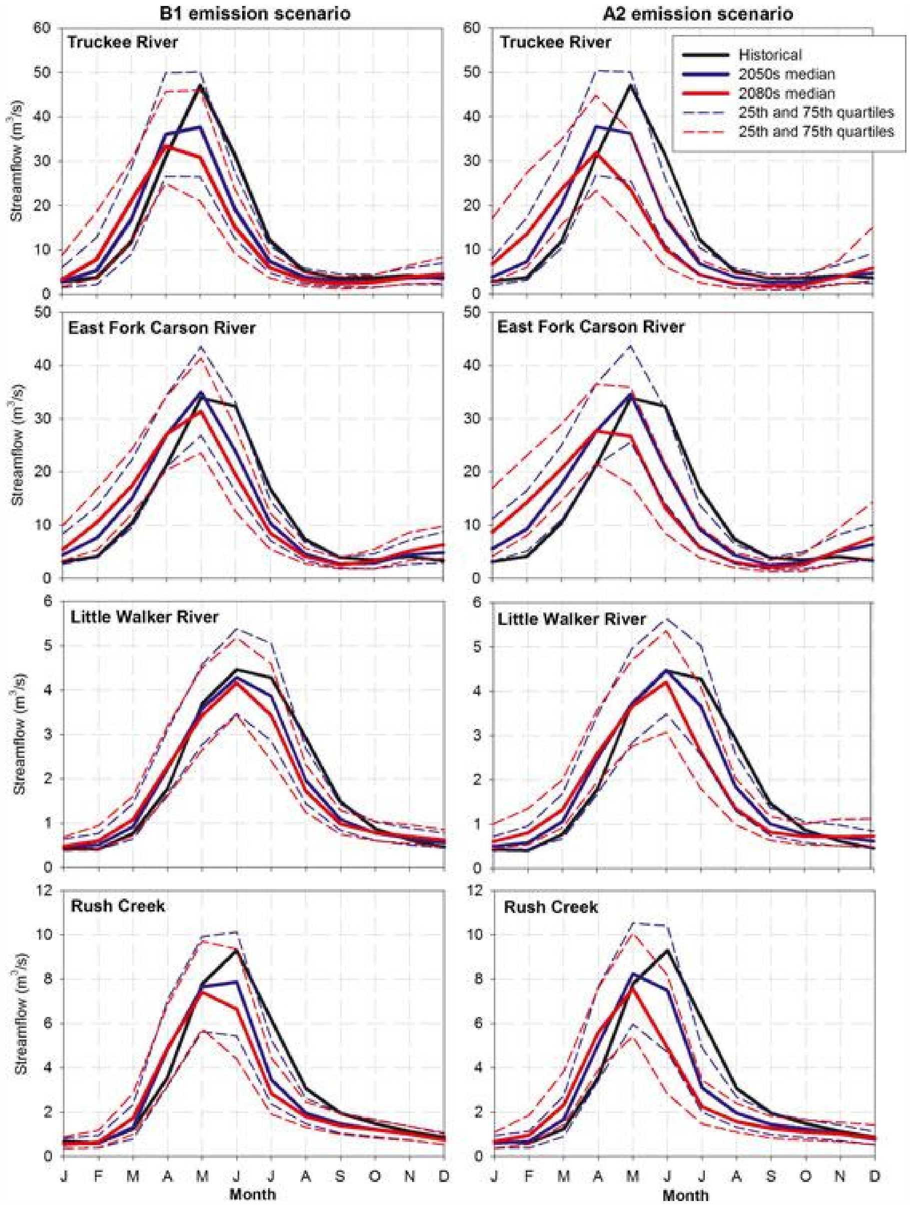

FIGURE 6. Average Median and Quartile Monthly Streamflow Projections for the 2050s and 2080s Under Each Emission Scenario for the Selected Eastern Sierra Nevada Watersheds.

watershed (1.58), Truckee River watershed (1.52), Rush Creek watershed (1.29), Sacramento River watershed (1.19), and American River watershed (1.02) (Figure 7). A statistically significant ($p < 0.05$) positive correlation of $\rho = 0.72$ was found between watershed sensitivity and median elevation, suggesting that watersheds containing high elevations (thus snow accumulation) are more sensitive to climate change that is primarily characterized by warming. Conversely, watersheds containing a large portion of lower elevations (and thus less or even no snow accumulation as previously discussed) can be expected to be less sensitive to changes in temperature.

Hydrologic Component Analysis

An increase in temperature coupled with a decrease in precipitation affected the seasonality and volumes of the different hydrologic components of streamflow throughout the Sierra Nevada (Figures 8 and 9). For the ensemble median, a decrease in total precipitation was found for all watersheds, with a larger decrease found during the summer months (~35% decrease compared with historical precipitation) when compared with the winter months (~15% decrease compared with historical precipitation). There was no discernable difference between precipitation changes

TABLE 5. Average Monthly Percent Change from the 2080s A2 Scenario to the Historical Time Period.

Watershed	Median (% change)	25th Percentile (% change)	75th Percentile (% change)
Kern River	−25.3	−61.8	33.7
San Joaquin River	−21.5	−52.4	27.4
Rush Creek	−20.6	−47.6	18.5
Truckee River	−19.1	−50.0	37.9
American River	−15.2	−53.0	43.7
Sacramento River	−12.1	−41.1	36.0
Little Walker River	−9.1*	−34.1	28.7
East Fork Carson River	−4.6*	−38.1	45.1

*Not significantly different at $\alpha = 0.05$.

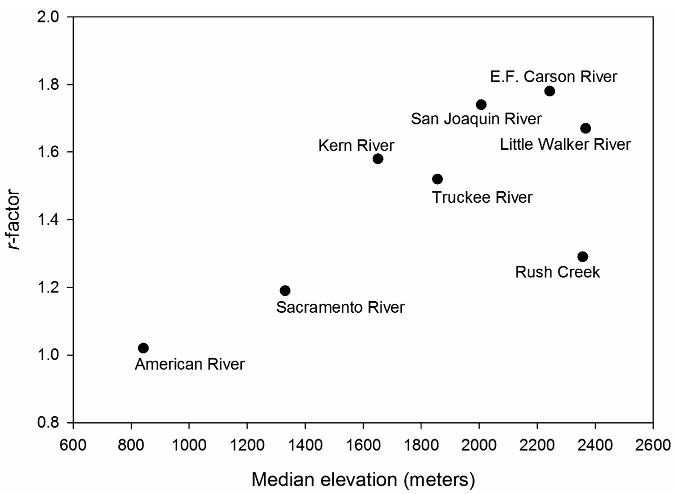

FIGURE 7. Scatterplot of Median Watershed Elevations and *r*-Factors of the Eight Major Sierra Nevada Watersheds.

for the western and eastern Sierra Nevada watersheds. However, the largest median decrease in precipitation occurred in the southern Sierra Nevada, as previously discussed. Peak snowmelt shifted to earlier in the year and the snowmelt runoff pulse decreased for both western and eastern watersheds. The magnitude of these changes, however, differed between the western and eastern sides. In the higher elevation eastern Sierra Nevada watersheds, the overall historic snowmelt contribution was advanced by up to two months and reduced by about 38% due to the median of projections indicating reduced precipitation. In spite of the overall decreases in the eastern Sierra Nevada, snowmelt during the 2080s is projected to be slightly higher than the historical time period during the months January and February, reflecting the timing shift in snowmelt that is also evident in Figure 6. By contrast, for the western Sierra Nevada watersheds, the initial snowmelt component varies with watershed elevation, but is generally lower than the eastern watersheds, and with warmer temperatures the snowmelt component is substantially diminished as well as advanced. Due to the large loss in the snowmelt component from the increase in temperature and decrease in precipitation, no increase of snowmelt for any month was found by the end of the century. These findings are in agreement with other studies (Miller *et al.*, 2003; Knowles and Cayan, 2004; Maurer, 2007; Young *et al.*, 2009) where the mid-range elevation (1,500 to 3,000 m) snowmelt is most affected by increases in temperature. The peak reductions are occurring in these mid-range elevations because they overall have less snow accumulation, whereas the higher elevations will potentially remain cold enough that temperature increases will have less of an effect (Young *et al.*, 2009).

A decrease in precipitation led to a decrease in surface runoff throughout the Sierra Nevada. Our results suggest that surface runoff is a minor component for the hydrologic cycle throughout the Sierra Nevada, and that, contrary to the findings of previous studies where surface runoff increased caused by the shift from snow to rain (e.g., Knowles *et al.*, 2006; Null *et al.*, 2010), the surface runoff contribution to streamflow from precipitation does not increase for any of the major Sierra Nevada watersheds. Additionally, peak surface runoff timing does not shift. Figures 8 and 9 show that even though there is a decrease in precipitation, annual soil water storage, which is the amount of water held within the soil column, is close to historical period volumes for some watersheds, indicating that the precipitation that is occurring is being infiltrated into the soil column, which may eventually contribute to subsurface flow. Therefore, the increase in surface runoff found in other studies is being infiltrated into the soil column in our study. Another interpretation is that even though surface runoff is a minor component of the hydrologic cycle, the decrease in water yield (or streamflow) coupled with invariant soil water volume is mainly from the decreased surface runoff. A combination of these interpretations may also be the cause of the decreased streamflow.

For the eastern Sierra Nevada, soil water storage peaks shift from April to March. Compared with the historical time period, soil water storage was lower in the spring and early summer and higher in the fall for the Truckee River, East Fork Carson River, and Little Walker River watersheds due to a decrease in surface runoff volume and approximately similar evapotranspiration. For the eastern and western Sierra Nevada watersheds, soil water storage is a large component of the hydrologic cycle. The soil water storage component in the western north Sierra Nevada watersheds is about twice the amount of the

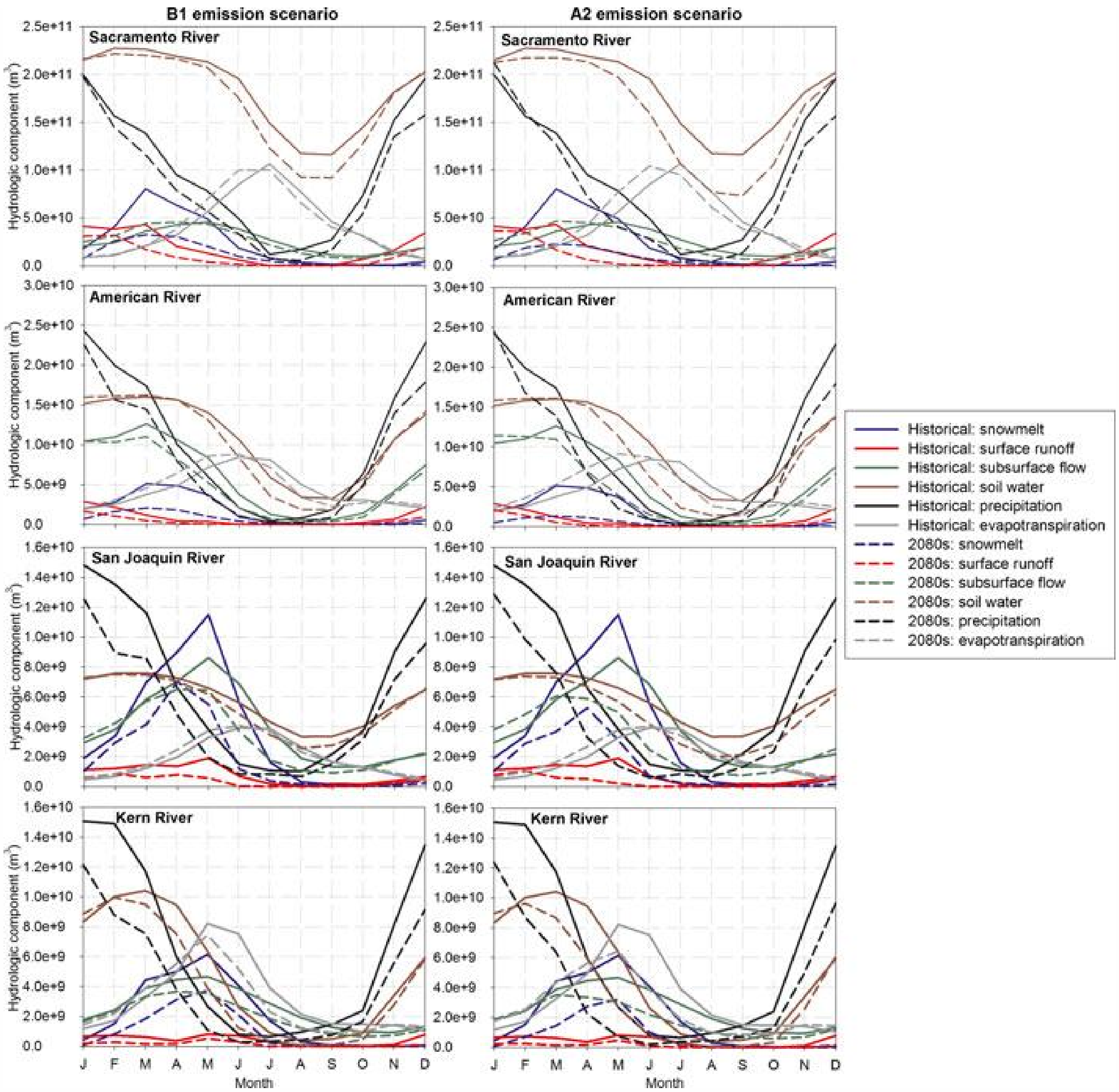

FIGURE 8. Total Hydrologic Component Volumes for the Selected Western Sierra Nevada Watershed for the 2080s Under Both Emission Scenarios.

snowmelt component during the historical and future climate scenarios. There was no apparent shift in soil water storage, with declines during the summer and fall. It should be noted that, in recent work (Maurer *et al.*, 2010b; Najafi *et al.*, 2011), the parameterization of soil moisture recharge in the chosen hydrologic model may influence the simulated sensitivity of some aspects of the hydrologic cycle, especially during low-flow periods, to climate changes. The western south Sierra Nevada soil water storage is approximately the same as the snowmelt component. For the Kern River watershed, soil water storage shifted from March to February, largely due to a decrease in surface runoff coupled with snowmelt volumes that were approximately similar to historical time period volumes.

Changes in soil water storage led to changes in subsurface streamflow contribution. The subsurface flow streamflow contribution follows the same trends as the other hydrologic components with changes in total contribution as well as peak shifts. For the eastern Sierra Nevada, the subsurface flow was less than the snowmelt component, with an earlier shift in peak subsurface flow of about one month. For the western Sierra Nevada, the magnitude of subsurface flow was generally the same as snowmelt, with declines in spring and early summer. A temporal advance in subsurface flow was also found throughout the western Sierra Nevada, where subsurface flow under climate change is higher than the historical time period for the late winter and early spring. The shifts found for the eastern Sierra Nevada and

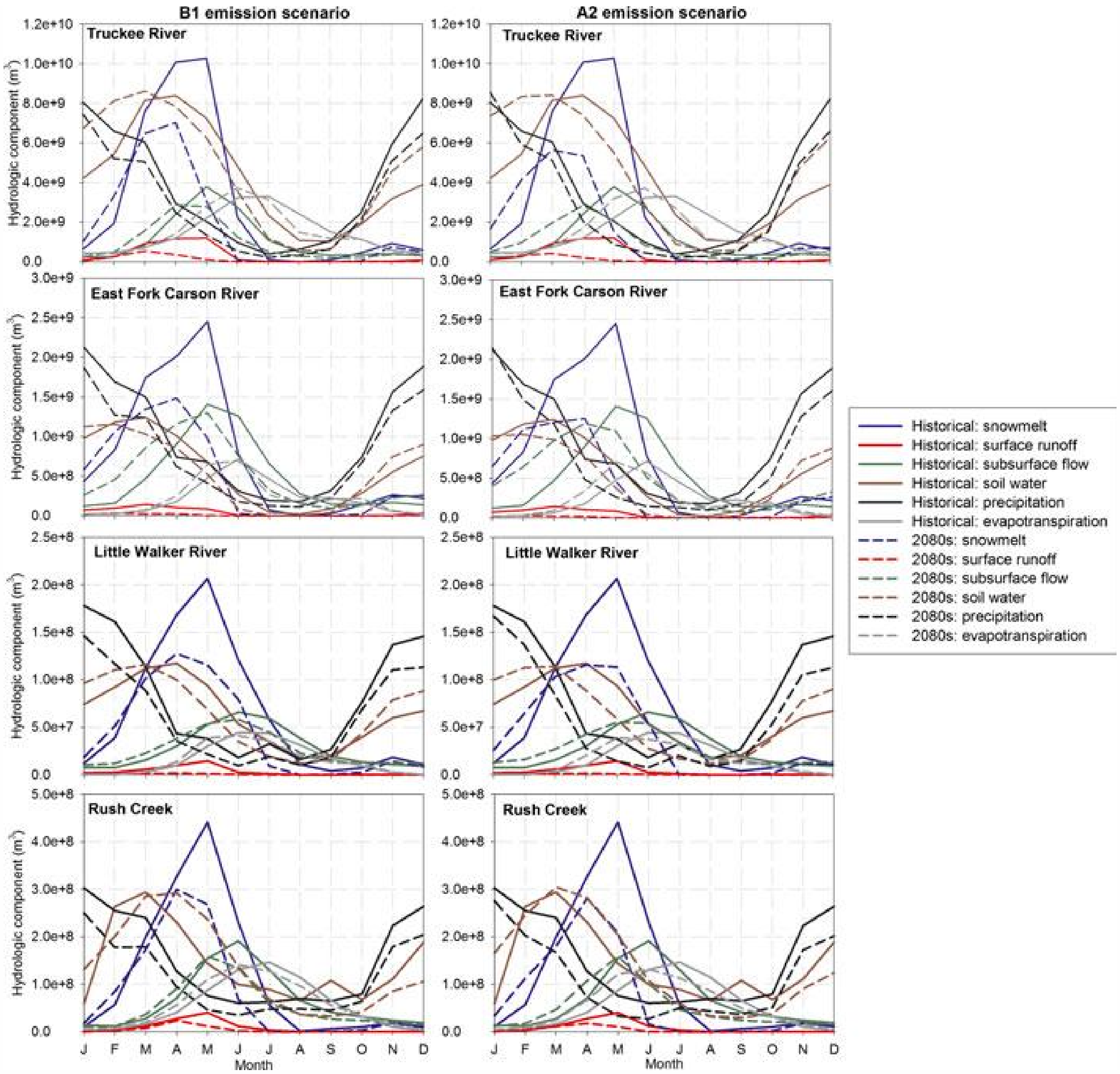

FIGURE 9. Total Hydrologic Component Volumes for the Selected Eastern Sierra Nevada Watershed for the 2080s Under Both Emission Scenarios.

Kern River watersheds were similar to results found in Eckhardt and Ulbrich (2003) for groundwater recharge, where groundwater recharge shifted due to changes in the snowmelt regime and a forward shift in plant growth.

Additionally, the timing of evapotranspiration is advanced by approximately one month throughout the Sierra Nevada. Therefore, the water held at the surface and the near-surface soil layers is being evaporated earlier in the year, leaving room for more water infiltration and less water available for plant growth. For the eastern and western Sierra Nevada, the overall magnitude of evapotranspiration under climate change remained approximately similar to the historical time period. The Kern River watershed, however, showed an overall decrease in evapotranspiration, resulting from a large decrease in precipitation coupled with an increase in temperature, resulting in less available water.

In summary, in spite of the differences in snowmelt contribution and shift between the eastern and western watersheds, the remaining hydrologic components exhibit similar changes in both regions. As subsurface flows and soil water storage shift to earlier in the season, these components decline for the spring and early summer. In addition, surface runoff flows, which are a small contributor to flows, decline during winter and spring, and the timing of evapotranspiration is shifted to earlier. Therefore, an earlier snowmelt impacts not only streamflow, but also evapotranspiration, surface, and subsurface flows, thus potentially impacting not only the immediate aquatic ecosystems but also the vegetation and thus terrestrial ecosystem within the watersheds.

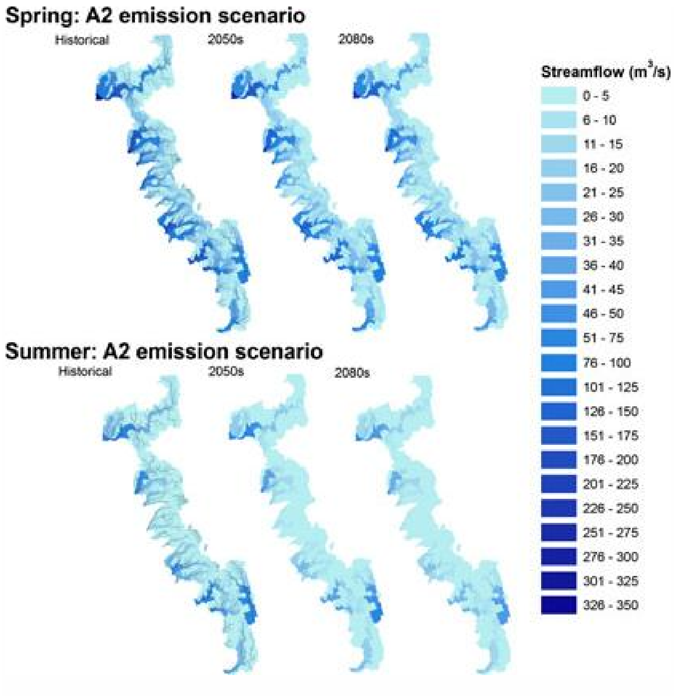

FIGURE 10. Spatial Average Median Streamflow Discharge for the Spring and Summer Seasons Under the A2 Emission Scenario.

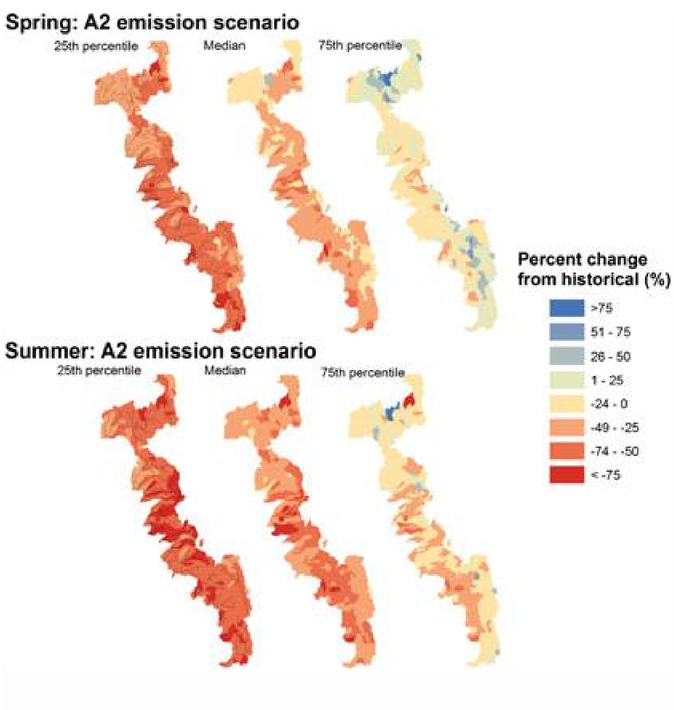

FIGURE 11. Spatial Average Median Streamflow Discharge Percent Changes for the Spring and Summer Seasons Under the A2 Emission Scenario.

Spatial Analysis for Streamflow Changes

From an ecological perspective, the high streamflow spring and low streamflow summer seasons are important for aquatic species and ecosystem health. Thus, it is of some importance to indentify where changes in these seasonal flows occur. Life cycles of aquatic species in the Sierra Nevada have evolved over thousands of years to match these wet and dry cycles (Erman, 1996), and changes in these cycles may have a significant effect on the health of aquatic species. For example, a decrease in summer streamflow coupled with an increase in air temperature will lead to an increase in water temperature, potentially decreasing suitable habitat. Figure 10 displays the average median spring and summer streamflow for the historical, 2050s, and 2080s for the A2 emission scenario, and Figure 11 shows the average seasonal change compared with the historical time period. For both seasons, there was a statistically significant ($p < 0.05$) positive correlation found between the 2080s A2 scenario median streamflow and subwatershed average elevation, as well as median streamflow and latitude. This suggests that there is significantly larger streamflow decreases at lower elevations, as well as larger streamflow decreases with a decrease in latitude.

For the spring season, the largest decreases are in the lower elevations in the central and southern Sierra Nevada for the median streamflow simulation of the 2080s (A2 scenario, Figure 11). The largest decreases were found in the Cosumnes River watershed, where the maximum elevation does not reach the Sierra Nevada crest and is thus more susceptible to earlier melting. The smallest spring streamflow changes (−25 to 25%) occur in the northern and southeastern Sierra Nevada, where for some subwatersheds, increases of spring streamflow occur. Over 90% of the subwatersheds show small decreases (−25 to +25%) throughout the Sierra Nevada for the spring 75th streamflow percentile. However, large decreases (−25 to −49%) are still found in the mid-range elevations of the central Sierra Nevada, which are the same regions projected to have large decreases in snowmelt.

Larger streamflow decreases are expected for the summer season compared with the spring season. Of the 498 modeled subwatersheds, summer streamflow is expected to decrease by more than 50% for 47% of the subwatersheds, compared with the 9% of the subwatersheds for the spring season. Similar to the spring season, the largest decreases (<−75%) are found at lower elevations in the central and southern Sierra Nevada. The projected summer 25th streamflow percentile shows large decreases in streamflow throughout the Sierra Nevada, whereas the 75th percentile shows moderate decreases (−49 to −25%) in the central and southern Sierra Nevada. The majority of subwatersheds for the 75th streamflow percentile fall within the −24 to 0% range, suggesting that, even under a "best-case" scenario, summer streamflow is likely to decrease throughout the Sierra Nevada.

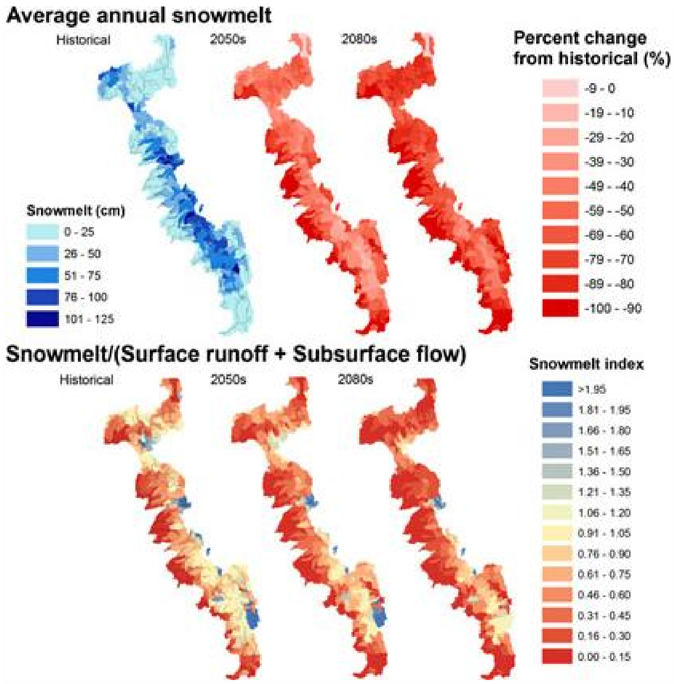

FIGURE 12. Percent Changes in Average Median Annual Snowmelt and Hydrologic Component Indices Under the A2 Emission Scenario.

Spatial Analysis for Snowmelt Changes

Projected changes in snowmelt exhibited great spatial heterogeneity (Figure 12). As expected, the largest snowmelt changes occur in the lower elevation watersheds. There was statistically significant ($p < 0.05$) correlation between subwatershed elevation and the percent change in snowmelt from the 2080s to the historical time period. From the 2050s to the 2080s, the percent change in snowmelt increases into the higher elevation subwatersheds. In the 2050s, approximately 62% of the subwatersheds decrease in snowmelt by more than 50%. In the 2080s, this value increases to 89% of the subwatersheds, demonstrating continuing widespread snowmelt decline.

A hydrologic component index (HCI) (average median annual snowmelt divided by the sum of surface runoff and subsurface flow) was utilized to analyze the relative shift in the roles of the hydrologic components to streamflow contribution. An HCI of 1 indicates equal streamflow contribution between snowmelt and surface runoff and subsurface flow. For the historical time period, HCI values >1 are concentrated in the higher elevation subwatersheds, signifying that snowmelt is a large part of streamflow contribution. From the historical period to the 2050s and 2080s, the HCI values decrease, indicating an increasing role of surface runoff and subsurface flow. There was statistically significant correlation ($p < 0.05$) between elevation and changes in HCI. For the eastern Sierra Nevada and some of the higher elevation subwatersheds, HCI values remain near 1, suggesting that snowmelt will still be a large portion of the streamflow under the warming projected by the end of the century.

CONCLUSIONS

As shifts in the hydrology that are expected from climatic changes may have serious impacts on water supplies and aquatic ecosystems in the Sierra Nevada, a systematic analysis of these changes on the subwatershed scale is presented here. Our study investigates the effect of climatic changes not only on snowmelt, precipitation, and streamflow, but also on the other hydrologic components of streamflow, such as surface runoff, subsurface flow, soil water storage, and evapotranspiration. To this end, a calibrated SWAT model was used to simulate the effects of climate change on Sierra Nevada hydrology using 16 GCMs with two emission scenarios. Temperatures are expected to increase, and although projected precipitation changes varied between GCMs, an overall decrease is expected.

Similar to other studies, our simulations suggest a continued future decrease in average median annual streamflow, as well as shift in monthly peak streamflow, throughout the Sierra Nevada. The largest streamflow reductions were found for the mid-range elevations of 1,500 to 3,000 m due to less initial snow accumulation and warmer spring temperatures, whereas the higher elevation subwatersheds are expected to remain more resilient due to colder temperatures. The high elevation East Fork Carson River and San Joaquin River watersheds were found to be the most sensitive to changes in climate based on the first and third projected streamflow quartiles.

Our simulations suggest that as peak snowmelt is expected to advance by several weeks, with an overall decrease in snowmelt volume, the remaining hydrologic flow components for the watersheds studied will likely be affected with potential ecological implications. Although annual soil water storage will likely remain near historical period volumes for some watersheds, the earlier snowmelt coupled with decreases in precipitation is projected to decrease soil storage in spring and summer. Differences in soil water storage between regions were largely due to changes in precipitation but also differences in physical soil properties. In addition to soil storage, surface and subsurface flow timing is expected to advance, with resulting declines in surface flows for winter and spring and subsurface flows for spring and early summer. Additionally, evapotranspiration annual volumes remained similar whereas the peak evapotranspiration advanced by one month. Thus, an earlier snowmelt affects not only streamflow, but also evapotranspiration, surface, and subsurface flows, thus potentially threatening not only the immediate aquatic ecosystems but also the vegetation and thus terrestrial ecosystem within the watersheds during times important for growth and reproduction.

Declining spring and summer flows did not equally affect all subwatersheds in the region, and the subwatershed perspective allowed for identification for the most sensitive basins throughout the Sierra Nevada. These findings could aid in ecosystem management decisions. Although flows during the spring season were decreased substantially for some watersheds, almost half of the subwatersheds in the Sierra Nevada exhibited substantial decreases for the summer season. Therefore, the largest changes are expected during the time of greatest water demand and lowest historical flows. Further reducing summer low flows might impact stream ecosystems through a combination of less available water and higher stream water temperatures, a particular concern for cold water species. The largest snowmelt changes occur in the higher elevations from the 2050s to the 2080s, and during this time period, surface runoff and subsurface streamflow contributions become increasingly more important to maintain streamflow volumes. Thus, as warming progresses, the eastern Sierra might become more vulnerable to climatic changes, as temperatures might warm sufficiently to significantly alter snowmelt timing and as these watersheds do not contain the soils or geologic material to absorb these earlier flows. It should be noted that this study assumed that land use and atmospheric CO_2 would not change for the duration of the simulations and that the simplified groundwater routine that is part of SWAT adequately determines groundwater flow volumes for this study.

This study presents one of the first climate change hydrologic analyses at the subwatershed scale in the Sierra Nevada, and has shown the changes in hydrology from changes in climate can vary greatly between subwatersheds. Knowledge of the magnitude and location of such changes will be important to water resources managers operating at scales smaller than the regional watershed.

ACKNOWLEDGMENTS

The authors gratefully acknowledge financial support for this work from the U.S. Environmental Protection Agency through EPA STAR Grant No. RD-83419101-0. We acknowledge the modeling groups, the Program for Climate Model Diagnosis and Intercomparison (PCMDI) and the WCRP's Working Group on Coupled Modelling (WGCM), for their roles in making available the WCRP CMIP3 multi-model dataset. Support of this dataset is provided by the Office of Science, U.S. Department of Energy.

LITERATURE CITED

Abbaspour, K.C., J. Yang, I. Maximov, R. Siber, K. Bogner, J. Mieleitner, J. Zobrist, and R. Srinivasan, 2007. Modelling Hydrology and Water Quality in the Pre-Alpine/Alpine Thur Watershed Using SWAT. Journal of Hydrology 333:413-430.

Arnold, J.G., R. Srinivasan, R.S. Muttiah, and J. R. Williams, 1998. Large Area Hydrologic Modeling and Assessment Part I: Model Development. Journal of the American Water Resources Association 34:73-89.

Barnett, T.P., J.C. Adam, and D.P. Lettenmaier, 2005. Potential Impacts of a Warming Climate on Water Availability in Snow-Dominated Regions. Nature 438:303-309, doi: 310.1038/nature04141.

Barnett, T.P., D.W. Pierce, H.G. Hidalgo, C. Bonfils, B.D. Santer, T. Das, G. Bala, A.W. Wood, T. Nozawa, A.A. Mirin, D.R. Cayan, and M.D. Dettinger, 2008. Human-Induced Changes in the Hydrology of the Western United States. Science 319:1080-1083, doi: 1010.1126/science.1152538.

Blumm, M. and T. Schwartz, 2003. Mono Lake and Evolving Public Trust in Western Water. Issues in Legal Scholarship 1:1-40.

Brekke, L.D., N.L. Miller, K.E. Bashford, N.W.T. Quinn, and J.A. Dracup, 2004. Climate Change Impacts Uncertainty for Water Resources in the San Joaquin River Basin, California. Journal of the American Water Resources Association 40:149-164.

Cayan, D.R., E.P. Maurer, M.D. Dettinger, M. Tyree, and K. Hayhoe, 2008. Climate Change Scenarios for the California Region. Climatic Change 87(Suppl. 1):21-42, doi: 10.1007/s10584-10007-19377-10586.

Christensen, J.H., B. Hewitson, A. Busuioc, A. Chen, X. Gao, I. Held, R. Jones, R.K. Kolli, W.-T. Kwon, R. Laprise, V. Magaña Rueda, L. Mearns, C.G. Menéndez, J. Räisänen, A. Rinke, A. Sarr, and P. Whetton, 2007. Regional Climate Projections. *In*: Climate Change 2007: The Physical Science Basis. Contribution of Working Group I to the Fourth Assessment Report of the Intergovernmental Panel on Climate Change, S. Solomon, D. Qin, M. Manning, Z. Chen, M. Marquis, K.B. Averyt, M. Tignor, and H.L. Miller (Editors). Cambridge University Press, Cambridge, United Kingdom and New York, pp. 847-940.

Coats, R., 2010. Climate Change in the Tahoe Basin: Regional Trends, Impacts and Drivers. Climatic Change 102:435-466.

Coats, R., M. Costa-Cabral, J. Riverson, J. Reuter, G. Sahoo, G. Schladow, and B. Wolfe, 2012. Projected 21st Century Trends in Hydroclimatology of the Tahoe Basin. Climatic Change, in press.

Conklin, M.H. and F. Liu, 2006. Groundwater Contributions to Baseflow in the Merced River: Processes, Flow Paths, and Residence Times. PIER Final Project Report CEC-500-2007-116, California Energy Commission, Sacramento, California.

Cook, E.R., R. Seager, M.A. Cane, and D.W. Stahle, 2007. North American Drought: Reconstructions, Causes, and Consequences. Earth Science Reviews 81:93-134.

Delworth, T.L., A.J. Broccoli, A. Rosati, R.J. Stouffer, V. Balaji, J.A. Beesley, W.F. Cooke, K.W. Dixon, J. Dunne, K.A. Dunne, J.W. Durachta, K.L. Findell, P. Ginoux, A. Gnanadesikan, C.T. Gordon, S.M. Griffies, R. Gudgel, M.J. Harrison, I.M. Held, R.S. Hemler, L.W. Horowitz, S.A. Klein, T.R. Knutson, P.J. Kushner, A.R. Langenhorst, H.-C. Lee, S.-J. Lin, J. Lu, S.L. Malyshev, P.C.D. Milly, V. Ramaswamy, J. Russell, M.D. Schwarzkopf, E.

Shevliakova, J.J. Sirutis, M.J. Spelman, W.F. Stern, M. Winton, A.T. Wittenberg, B. Wyman, F. Zeng, and R. Zhang, 2006. GFDL's CM2 Global Coupled Climate Models – Part 1: Formulation and Simulation Characteristics. Journal of Climate 19: 643-674.

Dettinger, M.D., 2005. From Climate-Change Spaghetti to Climate-Change Distributions for 21st Century California. San Francisco Estuary & Watershed Science 3:1-14.

Dettinger, M.D., D.R. Cayan, M. Meyer, and A.E. Jeton, 2004. Simulated Hydrologic Responses to Climate Variations and Change in the Merced, Carson, and American River Basins, Sierra Nevada, California, 1900-2099. Climatic Change 62: 283-317.

Diansky, N.A. and E.M. Volodin, 2002. Simulation of Present-Day Climate with a Coupled Atmosphere-Ocean General Circulation Model. Izvestiya, Atmospheric and Oceanic Physics (English Translation) 38:732-747.

Eckhardt, K. and U. Ulbrich, 2003. Potential Impacts of Climate Change on Groundwater Recharge and Streamflow in a Central European Low Mountain Range. Journal of Hydrology 284 (1-4):244-252.

Erman, N.A., 1996. Status of Aquatic Invertebrates. In Sierra Nevada Ecosystem Project: Final Report to Congress, Vol. II, Chap. 35. University of California, Centers for Water and Wildland Resources, Davis.

Erman, N.A and C.D. Nagano, 1992. A Review of the California Caddisflies (Trichoptera) Listed as Candidate Species on the 1989 Federal "Endangered and Threatened Wildlife and Plants: Animal Notice of Review." California Fish and Game 78(2): 45-56.

Ficklin, D.L., Y. Luo, E. Luedeling, S.E. Gatzke, and M. Zhang, 2009. Sensitivity of Agricultural Runoff to Rising Levels of CO_2 and Climate Change in the San Joaquin Valley Watershed of California. Environmental Pollution 158:223-234.

Ficklin, D.L., I.T. Stewart, and E.P. Maurer, 2012. Effects of Projected Climate Change on the Hydrology in the Mono Lake Basin. Climatic Change, in press.

Flato, G.M., and G.J. Boer, 2001. Warming Asymmetry in Climate Change Simulations. Geophysical Research Letters 28:195-198.

Fontaine, T.A., T.S. Cruickshank, J.G. Arnold, and R.H. Hotchkiss, 2002. Development of a Snowfall-Snowmelt Routine for Mountainous Terrain for the Soil and Water Assessment Tool (SWAT). Journal of Hydrology 262:209-223.

Furevik, T., M. Bentsen, H. Drange, I.K.T. Kindem, and N.G. Kvamstø, 2003. Description and Evaluation of the Bergen Climate Model: ARPEGE Coupled with MICOM. Climate Dynamics 21:27-51.

Gassman, P.W., M.R. Reyes, C.H. Green, and J.G. Arnold, 2007. The Soil and Water Assessment Tool: Historical Development, Applications, and Future Research Directions. Transactions of the American Society of Agricultural and Biological Engineers 50:1211-1250.

Gedney, N., P.M. Cox, R.A. Betts, O. Boucher, C. Huntingford, and P.A. Scott, 2006. Detection of a Direct Carbon Dioxide Effect in Continental Runoff Records. Nature 439:835-838.

Gleick, P.H. (Editor), 1993. Water in Crisis: A Guide to the World's Fresh Water Resources. Oxford University Press, New York.

Gleick, P.H. and E.L. Chalecki, 1999. The Impacts of Climatic Changes for Water Resources of the Colorado and Sacramento-San Joaquin River Basins. Journal of the American Water Resources Association 35(6):1429-1441.

Gordon, C., C. Cooper, C.A. Senior, H. Banks, J.M. Gregory, T.C. Johns, J.F.B. Mitchell, and R.A. Wood, 2000. The Simulation of SST, Sea Ice Extents and Ocean Heat Transports in a Version of the Hadley Centre Coupled Model Without Flux Adjustments. Climate Dynamics 16:147-168.

Gordon, H.B., L.D. Rotstayn, J.L. McGregor, M.R. Dix, E.A. Kowalczyk, S.P. O'Farrell, L.J. Waterman, A.C. Hirst, S.G. Wilson, M.A. Collier, I.G. Watterson, and T.I. Elliott, 2002. The CSIRO Mk3 Climate System Model, CSIRO Atmospheric Research Technical Paper No. 60. CSIRO. Division of Atmospheric Research, Victoria, Australia, p. 130.

Hanson, R.T., M.W. Newhouse, and M.D. Dettinger, 2004. A Methodology to Assess Relations Between Climatic Variability and Variations in Hydrologic Time Series in the Southwestern United States. Journal of Hydrology 287:252-269.

Hawkins, E. and R. Sutton, 2009. The Potential to Narrow Uncertainty in Regional Climate Predictions. Bulletin of the American Meteorological Society 90:1095-1107.

Hawkins, E. and R.T. Sutton, 2011. The Potential to Narrow Uncertainty in Projections of Regional Precipitation Change. Climate Dynamics 37(1-2):407-418.

Hayhoe, K., D. Cayan, C.B. Field, P.C. Frumhoff, E.P. Maurer, N.L. Miller, S.C. Moser, S.H. Schneider, K.N. Cahill, E.E. Cleland, L. Dale, R. Drapek, R.M. Hanemann, L.S. Kalkstein, J. Lenihan, C.K. Lunch, R.P. Neilson, S.C. Sheridan, and J.H. Verville, 2004. Emissions Pathways, Climate Change, and Impacts on California. Proceedings of the National Academy of Sciences 101:12422-12427.

Hershler, R., 1994. A Review of the North American Freshwater Snail Genus *Pyrgulopsis* (Hydrobiidae). Smithsonian Contributions to Zoology 554. Smithsonian Institution, Washington, D.C.

IPSL, 2005. The New IPSL Climate System Model: IPSL-CM4. Institut Pierre Simon Laplace des Sciences de l'Environnement Global, Paris, France, p. 73.

Jungclaus, J.H., M. Botzet, H. Haak, N. Keenlyside, J.-J. Luo, M. Latif, J. Marotzke, U. Mikolajewicz, and E. Roeckner, 2006. Ocean Circulation and Tropical Variability in the AOGCM ECHAM5/MPI-OM. Journal of Climate 19:3952-3972.

K-1 Model Developers, 2004. K-1 Coupled Model (MIROC) Description, K-1 Technical Report, 1. Center for Climate System Research, University of Tokyo, Tokyo, Japan, p. 34.

Kiehl, J.T., J.J. Hack, G.B. Bonan, B.B. Boville, D.L. Williamson, and P.J. Rasch, 1998. The National Center for Atmospheric Research Community Climate Model: CCM3. Journal of Climate 11:1131-1149.

Knowles, N. and D.R. Cayan, 2002. Potential Effects of Global Warming on the Sacramento/San Joaquin Watershed and the San Francisco Estuary. Geophysical Research Letter 29(18): 1891.

Knowles, N. and D.R. Cayan, 2004. Elevational Dependence of Projected Hydrologic Changes in the San Francisco Estuary and Watershed. Climatic Change 62:319-336.

Knowles, N., M. Dettinger, and D. Cayan, 2006. Trends in Snowfall Versus Rainfall for the Western United States. Journal of Climate 19:4545-4559.

Krause, P., D.P. Boyle, and F. Bäse, 2005. Comparison of Different Efficiency Criteria for Hydrological Model Assessment. Advances in Geosciences 5:89-97.

Legutke, S. and R. Voss, 1999. The Hamburg Atmosphere-Ocean Coupled Circulation Model ECHO-G, Technical Report, No. 18. German Climate Computer Centre (DKRZ), Hamburg, Germany, p. 62.

Lettenmaier, D.P. and T.Y. Gan, 1990. Hydrologic Sensitivities of the Sacramento-San Joaquin River Basin, California, to Global Warming. Water Resources Research 26:69-86.

Maurer, E.P., 2007. Uncertainty in Hydrologic Impacts of Climate Change in the Sierra Nevada, California Under Two Emissions Scenarios. Climatic Change 82:309-325, doi: 310.1007/s10584-10006-19180-10589.

Maurer, E.P., L.D. Brekke, and T. Pruitt, 2010b. Contrasting Lumped and Distributed Hydrology Models for Estimating

Climate Change Impacts on California Watersheds. Journal of the American Water Resources Association 46(5):1024-1035.

Maurer, E.P. and P.B. Duffy, 2005. Uncertainty in Projections of Streamflow Changes Due to Climate Change in California. Geophysical Research Letters 32:L03704, doi: 03710.01029/02004GL021462.

Maurer, E.P., H.G. Hidalgo, T. Das, M.D. Dettinger, and D.R. Cayan, 2010a. The Utility of Daily Large-Scale Climate Data in the Assessment of Climate Change Impacts on Daily Streamflow in California. Hydrology and Earth System Sciences 14:1125-1138, doi: 1110.5194/hess-1114-1125-2010.

Maurer, E.P., A.W. Wood, J.C. Adam, D.P. Lettenmaier, and B. Nijssen, 2002. A Long-Term Hydrologically-Based Data Set of Land Surface Fluxes and States for the Conterminous United States. Journal of Climate 15:3237-3251.

Medlyn, B.E., C.V.M. Barton, M.S.J. Broadmeadow, R. Ceulemans, P. De Angelis, M. Forstreuter, M. Freeman, S.B. Jackson, S. Kellomaki, E. Laitat, A. Rey, P. Roberntz, B.D. Sigurdsson, J. Strassemayer, K. Wang, P.S. Curtis, and P.G. Jarvis, 2001. Stomatal Conductance of Forest Species After Long-Term Exposure to Elevated CO_2 Concentrations: A Synthesis. New Phytologist 149:247-264.

Meehl, G.A., C. Covey, T. Delworth, M. Latif, B. McAvaney, J.F.B. Mitchell, R.J. Stouffer, and K.E. Taylor, 2007a. The WCRP CMIP3 Multimodel Dataset: A New Era in Climate Change Research. Bulletin of the American Meteorological Society 88:1383-1394.

Meehl, G.A., C. Tebaldi, H. Teng, and T.C. Peterson, 2007b. Current and Future U.S. Weather Extremes and El Niño. Geophysical Research Letters 34:L20704, doi: 20710.21029/22007GL031027.

Mehta, V.K., D.E. Rheinheimer, D. Yates, D.R. Purkey, J.H. Viers, C.A. Young, and J.F. Mount, 2011. Potential Impacts of Hydrology and Hydropower Production Under Climate Warming of the Sierra Nevada. Journal of Water and Climate Change 2(1): 29-43.

Miller, N.L., K.E. Bashford, and E. Strem, 2003. Potential Impacts of Climate Change on California Hydrology. Journal of the American Water Resources Association 39:771-784.

Monteith, J.I.L., 1965. Evaporation and Environment. Academic Press, New York.

Moriasi, D.N., J.G. Arnold, M.W.V. Liew, R.L. Bingner, R.D. Harmel, and T.L. Veith, 2007. Model Evaluation Guidelines for Systematic Quantification of Accuracy in Watershed Simulations. Transactions of the American Society of Agricultural and Biological Engineers 50:885-900.

Morison, J.I.L. and R.M. Gifford, 1983. Stomatal Sensitivity to Carbon Dioxide and Humidity. Plant Physiology 71:789-796.

Moss, R.H., J.A. Edmonds, K.A. Hibbard, M.R. Manning, S.K. Rose, D.P. van Vuuren, T.R. Carter, S. Emori, M. Kainuma, T. Kram, G.A. Meehl, J.F.B. Mitchell, N. Nakicenovic, K. Riahi, S.J. Smith, R.J. Stouffer, A.M. Thomson, J.P. Weyant, and T.J. Wilbanks, 2010. The Next Generation of Scenarios for Climate Change Research and Assessment. Nature 463:747-756.

Najafi, M., H. Moradkhani, and I. Jung, 2011. Assessing the Uncertainties of Hydrologic Model Selection in Climate Change Impact Studies. Hydrologic Processes 25(18):2814-2826.

Nash, J.E. and J.V. Sutcliffe, 1970. River Flow Forecasting Through Conceptual Models Part I – A Discussion of Principles. Journal of Hydrology 10:282-290.

Neitsch, S.L., J.G. Arnold, J.R. Kiniry, J.R. Williams, and K.W. King, 2005. Soil and Water Assessment Tool Theoretical Documentation: Version 2005. Texas Water Resources Institute, College Station, Texas.

Null, S.E., J.H. Viers, and J.F. Mount, 2010. Hydrologic Response and Watershed Sensitivity to Climate Warming in California's Sierra Nevada. PLoS ONE 5:e9932.

Penman, H.L., 1956. Evaporation: An Introductory Survey. Netherlands Journal of Agricultural Science 9-29:87-97, 151-153.

Ralph, F.M. and M.D. Dettinger, 2011. Storms, Floods, and the Science of Atmospheric Rivers. Eos 92(32):265-266.

Raupach, M.R., G. Marland, P. Ciais, C. Le Quéré, J.G. Canadell, G. Klepper, and C.B. Field, 2007. Global and Regional Drivers of Accelerating CO_2 Emissions. Proceedings of the National Academy of Sciences 104(42):10288-10293.

Roe, G.H. and M.B. Baker, 2007. Why Is Climate Sensitivity So Unpredictable? Science 318:629-632.

Russell, G.L., J.R. Miller, D. Rind, R.A. Ruedy, G.A. Schmidt, and S. Sheth, 2000. Comparison of Model and Observed Regional Temperature Changes During the Past 40 Years. Journal of Geophysical Research-Atmospheres 105:14891-14898.

Russell, G.L., and D. Rind, 1999. Response to CO_2 Transient Increase in the GISS Coupled Model: Regional Coolings in a Warming Climate. Journal of Climate 12:531-539.

Salas-Mélia, D., F. Chauvin, M. Déqué, H. Douville, J.F. Gueremy, P. Marquet, S. Planton, J.F. Royer, and S. Tyteca, 2005. Description and Validation of the CNRM-CM3 Global Coupled Model, CNRM Working Note 103. Centre National de Recherches Météorologiques, Météo-France, Toulouse, France, p. 36.

Sanderson, B.M., C. Piani, W.J. Ingram, D.A. Stone, and M.R. Allen, 2007. Toward Constraining Climate Sensitivity by Linear Analysis of Feedback Patterns in Thousands of Perturbed-Physics GCM Simulations. Climate Dynamics 30:175-190.

SCS, 1984. SCS National Engineering Handbook. U.S. Department of Agriculture, Washington, D.C.

Stewart, I.T., D.R. Cayan, and M.D. Dettinger, 2004. Changes in Snowmelt Runoff Timing in Western North America Under a 'Business As Usual' Climate Change Scenario. Climatic Change 62:217-232.

Stewart, I.T., D.R. Cayan, and M.D. Dettinger, 2005. Changes Toward Earlier Streamflow Timing Across Western North America. Journal of Climate 18:1136-1155.

Tanaka, S.K., T. Zhu, J.R. Lund, R.E. Howitt, M.W. Jenkins, M.A. Pulido, M. Tauber, R.S. Ritzema, and I.C. Ferreira, 2006. Climate Warming and Water Management Adaptation for California. Climatic Change 76:361-387.

USDA-SCS (U.S. Department of Agriculture-Soil Conservation Service), 1993. State Soil Geographic Data Base (STATSGO). Miscellaneous Publication No. 1492, U.S. Government Printing Office, Washington, D.C.

USGS, 2007. NLCD 2001 Land Dover. U.S. Geological Survey, Sioux Falls, South Dakota.

Van Rheenen, N.T., A.W. Wood, R.N. Palmer, and D.P. Lettenmaier, 2004. Potential Implications of PCM Climate Change Scenarios for Sacramento-San Joaquin River Basin Hydrology and Water Resources. Climatic Change 62:257-281.

Vicuna, S., E.P. Maurer, B. Joyce, J.A. Dracup, and D. Purkey, 2007. The Sensitivity of California Water Resources to Climate Change Scenarios. Journal of the American Water Resources Association 43:482-498, doi: 410.1111/j.1752-1688.2007.00038.x.

Washington, W.M., J.W. Weatherly, G.A. Meehl, A.J. Semtner, T.W. Bettge, A.P. Craig, W.G. Strand, J. Arblaster, V.B. Wayland, R. James, and Y. Zhang, 2000. Parallel Climate Model (PCM) Control and Transient Simulations. Climate Dynamics 16:755-774.

Wiggins, G.B., 1990. Systematics of North American Trichoptera: Present Status and Future Prospects. *In*: Systematics of the North American Insects and Arachnids: Status and Needs, M. Kosztarab and C.W. Schaefer (Editors). Virginia Polytechnic Institute and State University, Agricultural Experiment Station, Blacksburg, Virginia, pp. 203-210.

Wigley, T.M.L. and P.D. Jones, 1985. Influences of Precipitation Changes and Direct CO_2 Effects on Streamflow. Nature 314:149-152.

Wood, A.W., L.R. Leung, V. Sridhar, and D.P. Lettenmaier, 2004. Hydrologic Implications of Dynamical and Statistical Approaches to Downscaling Climate Model Outputs. Climatic Change 62:189-216.

Wood, A.W., E.P. Maurer, A. Kumar, and D.P. Lettenmaier, 2002. Long-Range Experimental Hydrologic Forecasting for the Eastern United States. Journal of Geophysical Research-Atmospheres 107:4429, doi: 4410.1029/2001JD000659.

Young, C.A., M.I. Escobar-Arias, M. Fernandes, B. Joyce, M. Kiparsky, J.F. Mount, V.K. Mehta, D. Purkey, J.H. Viers, and D. Yates, 2009. Modeling the Hydrology of Climate Change in California's Sierra Nevada for Subwatershed Scale Adaptation. Journal of the American Water Resources Association 46(6):1409-1423.

Yukimoto, S., A. Noda, A. Kitoh, M. Sugi, Y. Kitamura, M. Hosaka, K. Shibata, S. Maeda, and T. Uchiyama, 2001. The New Meteorological Research Institute Coupled GCM (MRI-CGCM2), Model Climate and Variability. Papers in Meteorology and Geophysics 51:47-88.

Zhu, T., M.W. Jenkins, and J.R. Lund, 2005. Estimated Impacts of Climate Warming on California Water Availability Under Twelve Future Climate Scenarios. Journal of the American Water Resources Association 41:1027-1038.